AGU PUBLICATIONS

Global Biogeochemical Cycles

RESEARCH ARTICLE
10.1002/2015GB005090

Key Points:
- Significant diazotrophic community in both North and South Atlantic
- SST and pCO_2 have limited roles in diazotroph biogeography of tropical Atlantic
- Combined effects of Fe and P control diazotrophy in (sub)tropical Atlantic

Correspondence to:
J. T. Snow,
j.snow@noc.soton.ac.uk

Citation:
Snow, J. T., C. Schlosser, E. M. S. Woodward, M. M. Mills, E. P. Achterberg, C. Mahaffey, T. S. Bibby, and C. M. Moore (2015), Environmental controls on the biogeography of diazotrophy and *Trichodesmium* in the Atlantic Ocean, *Global Biogeochem. Cycles*, *29*, 865–884, doi:10.1002/2015GB005090.

Received 7 JAN 2015
Accepted 19 MAY 2015
Accepted article online 23 MAY 2015
Published online 26 JUN 2015

©2015. American Geophysical Union. All Rights Reserved.

Environmental controls on the biogeography of diazotrophy and *Trichodesmium* in the Atlantic Ocean

J. T. Snow[1], C. Schlosser[1,2], E. M. S. Woodward[3], M. M. Mills[4], E. P. Achterberg[1,2], C. Mahaffey[5], T. S. Bibby[1], and C. M. Moore[1]

[1]Ocean and Earth Science, University of Southampton, National Oceanography Centre, Southampton, UK, [2]GEOMAR Helmholtz-Zentrum für Ozeanforschung, Kiel, Germany, [3]Plymouth Marine Laboratory, Plymouth, UK, [4]Department of Earth System Science, Stanford University, Stanford, California, USA, [5]Department of Earth, Ocean and Ecological Sciences, School of Environmental Sciences, University of Liverpool, Liverpool, UK

Abstract The cyanobacterium *Trichodesmium* is responsible for a significant proportion of the annual "new" nitrogen introduced into the global ocean. Despite being arguably the best studied marine diazotroph, the factors controlling the distribution and growth of *Trichodesmium* remain a subject of debate, with sea surface temperature, the partial pressure of CO_2, and nutrients including iron (Fe) and phosphorus (P), all suggested to be important. Synthesizing data from seven cruises collectively spanning large temporal and spatial scales across the Atlantic Ocean, including two previously unreported studies crossing the largely undersampled South Atlantic gyre, we assessed the relationship between proposed environmental drivers and both community N_2 fixation rates and the distribution of *Trichodesmium*. Simple linear regression analysis would suggest no relationship between any of the sampled environmental variables and N_2 fixation rates. However, considering the concentrations of iron and phosphorus together within a simplified resource-ratio framework, illustrated using an idealized numerical model, indicates the combined effects these nutrients have on *Trichodesmium* and broader diazotroph biogeography, alongside the reciprocal maintenance of different biogeographic provinces of the (sub)tropical Atlantic in states of Fe or P oligotrophy by diazotrophy. The qualitative principles of the resource-ratio framework are argued to be consistent with both the previously described North-South Atlantic contrast in *Trichodesmium* abundance and the presence and consequence of a substantial non-*Trichodesmium* diazotrophic community in the western South Atlantic subtropical gyre. A comprehensive, observation-based explanation of the interactions between *Trichodesmium* and the wider diazotrophic community with iron and phosphorus in the Atlantic Ocean is thus revealed.

1. Introduction

Nitrogen (N_2) fixation by diazotrophs is a crucial component of the global nitrogen cycle and is ultimately responsible for the coupling of the marine nitrogen and phosphorous cycles and the maintenance of oceanic productivity [*Falkowski*, 1997]. *Trichodesmium*, a colonial, diazotrophic, cyanobacterium, has been a major focus of research due to the importance of this organism in influencing the nutrient biogeochemistry of the tropical and subtropical ocean [*Sohm et al.*, 2011b]. With an estimated 22 Tg N yr^{-1} fixed by *Trichodesmium* in the North Atlantic alone, this diazotrophic population contributes significantly to annual marine N_2 fixation (~80–200 Tg N yr^{-1}) [*Capone et al.*, 2005; *Mahaffey et al.*, 2005; *Duce et al.*, 2008]. However, recent work has emphasized the presence and importance of non-*Trichodesmium* diazotrophy in a range of environments [*Moisander et al.*, 2010; *Zehr*, 2011]. The balance of different environmental controls on the growth and biogeography of *Trichodesmium*, and diazotrophs in general, remains a matter of debate. Sea surface temperature (SST), pCO_2, and nutrients have all been suggested to be important drivers of diazotrophic activity, growth, and hence biogeography [*LaRoche and Breitbarth*, 2005; *Kranz et al.*, 2009, 2010; *Hutchins et al.*, 2013; *Fu et al.*, 2014]. However, the relative roles of these different drivers on diazotrophy in the modern ocean remain unclear [*Luo et al.*, 2013], significantly limiting our ability to project the future influence of this process on global biogeochemical cycles [*Boyd et al.*, 2010; *Moore et al.*, 2013] or to fully interpret the significant variability in oceanic N_2 fixation which appears to have occurred in the past [*Straub et al.*, 2013].

Natural populations of *Trichodesmium* are frequently argued to be physiologically constrained to the SST range of ~18–34°C, in large part due to correlative abundance observations [*LaRoche and Breitbarth*, 2005]. However, culture strains of *Trichodesmium* have also been shown to grow optimally at 24–30°C [*Breitbarth et al.*, 2007; *Fu et al.*, 2014]. Other diazotrophs, including heterocystous cyanobacteria, are prevalent in much colder environments, suggesting that elevated temperatures are not a de facto prerequisite for diazotrophic growth [*Staal et al.*, 2003; *Pandey et al.*, 2004; *Stal*, 2009]. Indeed, unicellular diazotrophs can be more abundant than *Trichodesmium* at lower temperatures in some regions [*Moisander et al.*, 2010]. Although the evolutionary time scales of temperature adaptation, both in situ and in culture, are largely unknown [*Huertas et al.*, 2011; *Thomas et al.*, 2012], phytoplankton appear to retain temperature optima reflecting that of their isolation environment [*Thomas et al.*, 2012]. Covariability of temperature with other environmental drivers in oceanic systems, including nutrient availability and water column stratification, consequently means that direct temperature constraints on diazotroph biogeography need to be considered alongside the potential for secondary adaptation to conditions found within the realized niche [*Monteiro et al.*, 2011; *Dutkiewicz et al.*, 2012; *Ward et al.*, 2013; *Dutkiewicz et al.*, 2014; *Fu et al.*, 2014].

Numerous *Trichodesmium* isolates and other diazotrophic taxa have been shown to have increased rates of N_2 and CO_2 fixation when cultured at elevated pCO_2 (e.g., current to projected end-of-century levels of ~750–1000 ppm), particularly when compared to preindustrial or Pleistocene glacial pCO_2 concentrations [*Barcelos e Ramos et al.*, 2007; *Hutchins et al.*, 2007; *Garcia et al.*, 2013; *Hutchins et al.*, 2013]. Sensitivities vary between strains [*Hutchins et al.*, 2013], with experimental doubling in pCO_2 typically increasing N_2 fixation rates by 35–100% [*Barcelos e Ramos et al.*, 2007; *Hutchins et al.*, 2007, 2013]. However, similar studies on natural *Trichodesmium* colonies have so far failed to show any such consistent effect [*Böttjer et al.*, 2014; *Gradoville et al.*, 2014]. Current geographical variability in surface water pCO_2 is also substantially less than the projected differences between contemporary ocean and glacial or end of century values [*Rödenbeck et al.*, 2013], suggesting that any pCO_2 sensitivity may be unlikely to exert a significant control on contemporary diazotroph biogeography.

Investigations into the nutritional requirements of *Trichodesmium* and other diazotrophs have focused on the requirements for iron (Fe) and phosphorus (P), with a number of novel nutrient acquisition and utilization strategies for Fe and P having been described [*Dyhrman et al.*, 2006; *Shi et al.*, 2007; *Orchard et al.*, 2009, 2010; *Richier et al.*, 2012]. *Trichodesmium* spp. are capable of accessing dissolved inorganic phosphorus (DIP) as PO_4^{3-} and dissolved organic phosphorus (DOP), in the form of both phosphomonoesters and phosphonates, which may be less widely bioavailable to the general microbial population [*Roy et al.*, 1982; *Dyhrman et al.*, 2006; *Sohm et al.*, 2008; *Orchard et al.*, 2009, 2010]. Recent work has also demonstrated that *Trichodesmium* structural P requirements can be reduced under conditions of low phosphorus availability via replacement of phospholipids for sulpholipids [*Van Mooy et al.*, 2009].

The presence of Fe within nitrogenase is expected to impose an enhanced diazotrophic requirement for this element [*Raven*, 1988]. In contrast to other diazotrophic cyanobacteria, which can reduce the instantaneous Fe burden through temporal separation of the two iron-rich metabolic processes of CO_2 and N_2 fixation [*Saito et al.*, 2011], *Trichodesmium* fixes both CO_2 and N_2 during the day through a complex combination of temporal and spatial segregation [*Berman-Frank et al.*, 2001; *Sandh et al.*, 2009]. Consequently, Fe requirements may be further enhanced for *Trichodesmium* as compared to the wider diazotrophic community [*Berman-Frank et al.*, 2007; *Richier et al.*, 2012].

The interface between the North Atlantic subtropical gyre (NASG) and the South Atlantic subtropical gyre (SASG) has repeatedly been noted as an environment characterized by high N_2 fixation rates and abundant *Trichodesmium* populations which can dominate the regional diazotrophic community [*Tyrrell et al.*, 2003; *Carpenter et al.*, 2004; *Capone et al.*, 2005; *Moore et al.*, 2009; *Großkopf et al.*, 2012]. Dissolved inorganic nitrogen (DIN) concentrations are persistently low and have been repeatedly demonstrated to proximally limit the abundance and activity of the nondiazotrophic community throughout the low-latitude oligotrophic Atlantic [*Ryther and Dunstan*, 1971; *Graziano et al.*, 1996; *Mills et al.*, 2004; *Moore et al.*, 2009]. In contrast, the concentration of DIP is significantly lower in the NASG when compared to the SASG [*Moore et al.*, 2009], as is evident from the SASG's elevated P* (where $P^* = DIP - DIN/16$) [*Deutsch et al.*, 2007]. Similarly, DOP and DOP* are also elevated in the SASG relative to the NASG [*Moore et al.*, 2009]. In contrast, surface water dissolved iron (DFe) concentrations are higher in the NASG than in

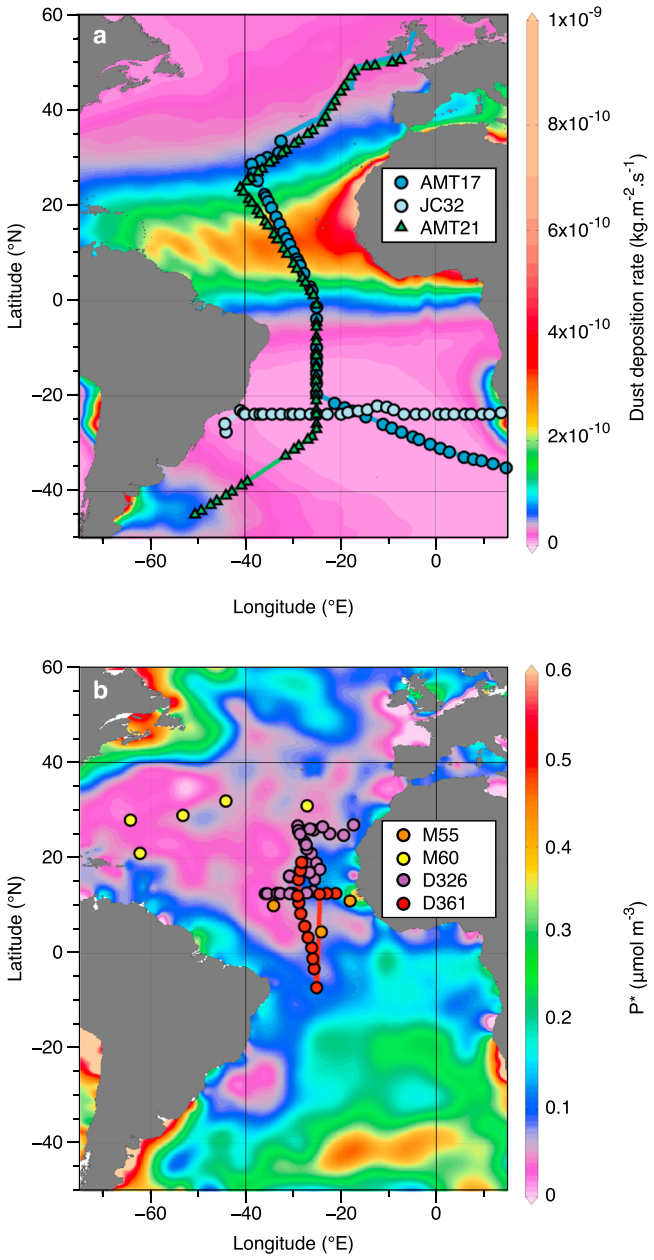

Figure 1. Cruise transects for the seven cruises included in this study. Transects are overlaid on (a) the modeled annual average dust deposition rate (kg m^{-2} s^{-1}) replotted from *Mahowald et al.* [2005] or (b) P* = DIP − DIN/16 from the World Ocean Circulation Experiment Ocean Atlas. Cruises are separated across maps for clarity.

the SASG due to atmospheric deposition of iron-rich Saharan dust into the former (Figure 1) [*Bowie et al.*, 2002; *Jickells et al.*, 2005; *Conway and John*, 2014].

The Intertropical Convergence Zone (ITCZ) is a significant contributor to the gradient in atmospheric deposition, shielding the South Atlantic from the high dust air masses of the northern hemisphere [*Schlosser et al.*, 2014]. Observed high rates of N_2 fixation have been ascribed to the ITCZ and Saharan dust-associated supplies of DFe [*Moore et al.*, 2009; *Schlosser et al.*, 2014] (Figure 1), which in turn depletes both DIP and DOP pools of the NASG, subsequently driving P availability down to the point where it may limit further diazotrophic growth [*Wu et al.*, 2000; *Moore et al.*, 2009]. Consequently, the resupply of DIP, DOP, or collectively total dissolved phosphorus (TDP) to the NASG via lateral advection of high P* and/or $DOP^{(*)}$ water may potentially become the controlling factor on diazotrophy in this system [*Mather et al.*, 2008; *Moore et al.*, 2009; *Palter et al.*, 2010; *Straub et al.*, 2013]. Moreover, the low P availability in the NASG, argued to result from diazotrophy [*Wu et al.*, 2000; *Moore et al.*, 2009], also results in P stress within the nondiazotroph community [*Lomas et al.*, 2010; *McLaughlin et al.*, 2013] despite N appearing to remain the proximal limiting nutrient [*Ryther and Dunstan*, 1971; *Graziano et al.*, 1996; *Moore et al.*, 2006].

In contrast to high rates of diazotrophy within the intergyre transition zone [*Moore et al.*, 2009; *Schlosser et al.*, 2014] and P limitation in the NASG [*Wu et al.*, 2000; *Sañudo-Wilhelmy et al.*, 2001], reported rates of diazotrophy are typically low within the SASG, presumably as a result of low Fe availability [*Moore et al.*, 2009; *Sohm et al.*, 2011c]. However, despite the SASG being broadly characterized by higher surface DIP (and hence P*) than the NASG, a marked region of low surface P* can be observed on the western side of the southern gyre [*Deutsch et al.*, 2007; *Moore et al.*, 2009]. Moreover, recent observations of H_2 supersaturation have been interpreted to result from significant diazotrophy in this region [*Moore et al.*, 2014].

Understanding extant environmental controls on diazotrophy is particularly important in the context of global change. Changes in SST, pCO_2, dust-driven iron fertilization, and physical excess P (re)supply have

all been hypothesized to potentially influence rates of N_2 fixation, resulting in possible shifts in the balance between local and global N_2 fixation and denitrification [*Falkowski*, 1997; *Breitbarth et al.*, 2007; *Moore et al.*, 2009; *Hutchins et al.*, 2013; *Straub et al.*, 2013; *Weber and Deutsch*, 2014]. The biological processes of N_2 fixation and denitrification, alongside other more minor sources and sinks, must ultimately balance out over sufficiently large time and space scales, in order to prevent the oceanic system from rapidly losing or gaining fixed nitrogen, which would significantly influence oceanic productivity and ultimately atmospheric pCO_2 [*Falkowski*, 1997; *Broecker and Henderson*, 1998; *Gruber*, 2008]. Identifying the scales over which this balance operates and hence establishing the associated time scale and strength of the coupling between the P and N cycles is crucial for understanding the controls on the oceanic N inventory and ultimately the potential for this to alter climate [*Falkowski*, 1997; *Straub et al.*, 2013; *Weber and Deutsch*, 2014].

In the current study we assembled a data set of *Trichodesmium* abundances and community N_2 fixation rates measured alongside hypothesized environmental drivers, collected during seven oceanic cruises using broadly consistent methodologies over the period of 2002–2011. Using this comprehensive data set we aim to assess the hypothesized importance of temperature, pCO_2, Fe, and P variability on the distribution of whole community N_2 fixation and *Trichodesmium* in particular. Utilizing concepts from resource-ratio theory [*Tilman*, 1980; *Tilman et al.*, 1982; *Ward et al.*, 2013], our interpretation of observed nutrient (Fe and P) patterns explicitly recognizes that limiting nutrient concentrations must reflect the end result of feedback within the nutrient microbial system, rather than being one-way drivers of microbial activity [*Cullen*, 1991; *Ward et al.*, 2013]. The analyzed data set thus enabled simultaneous investigation of a full suite of proposed environmental drivers of community diazotrophy and *Trichodesmium* biogeography in a region of pronounced environmental and diazotrophic gradients.

2. Methods

2.1. Sampling and Hydrography

Sampling was conducted during seven oceanic cruises: M55 (October to November 2002, R/V *Meteor*) [*Mills et al.*, 2004], M60 (March to April 2004, R/V *Meteor*) [*Moore et al.*, 2006, 2008], AMT17 (October to November 2005, RRS *Discovery*) [*Moore et al.*, 2009], D326 (January to February 2008, RRS *Discovery*) [*Richier et al.*, 2012], JC32 (March to May 2009, RRS *James Cook*), D361 (February to March 2011, RRS *Discovery*) [*Schlosser et al.*, 2014], and AMT21 (October to November 2011, RRS *Discovery*) (Figure 1). AMT17, D361, and AMT21 followed a north-south transect approximately along the 25°W meridian, as such data from these cruises will first be considered in a meridional context. M55, M60, D326, and JC32 covered a broader longitudinal area. Data from JC32 and AMT21 were previously unreported, while additional data beyond that already published are presented for D326 and D361.

Precipitation information sourced from the National Centers for Environmental Prediction (NCEP) Reanalysis data provided by NOAA/OAR/ESRL PSD, Boulder, Colorado, USA, (http://www.esrl.noaa.gov/psd/) was used as a proxy for the location and seasonality of the ITCZ. We have defined the ITCZ's location during D361 (representative of north hemisphere spring), AMT21 and AMT17 (representative of north hemisphere autumn) as the area where the surface precipitation flux was $>2\times10^{-5}\,\mathrm{kg\,m^{-2}\,s^{-1}}$.

2.2. DIN, DIP, DOP, and DFe

During cruises M55, M60, JC32, and AMT21, nitrate (NO_3^-), analyzed as nitrate + nitrite, nitrite (NO_2^-), and phosphate (PO_4^{3-}) were measured using a Bran and Luebbe AAIII segmented flow, colorimetric, autoanalyzer, or similar instrument using standard colorimetric techniques [*Brewer and Riley*, 1965; *Grasshoff et al.*, 1976]. For cruises D326, D361, and AMT17, nanomolar NO_3^-, NO_2^-, and PO_4^{3-} concentrations were determined with standard methods using segmented flow analysis with 2 m liquid waveguide capillary cells, [*Schlosser et al.*, 2014] for D361 and AMT21 and [*Patey et al.*, 2008] for D326. TDP concentrations were determined during cruises AMT17 [*Moore et al.*, 2009], D326 [*Mahaffey et al.*, 2014], and D361 [*Reynolds et al.*, 2014] by UV oxidation as previously described [*Moore et al.*, 2009; *Reynolds et al.*, 2014]. DOP concentrations were calculated as the difference in phosphate concentration before (DIP) and after (TDP) UV oxidation of seawater samples (i.e., DOP = TDP − DIP).

DFe concentrations were determined from surface water samples collected during M55 [*Croot et al.*, 2004], M60, AMT17 [*Moore et al.*, 2009], D326 [*Rijkenberg et al.*, 2012], D361 [*Schlosser et al.*, 2014], and AMT21

using a trace metal clean towed fish or titanium-framed conductivity-temperature-depth. Samples were filtered using 0.2 μm cartridge filters (Acropak/Sartobran P300 or similar) and acidified with ultraclean grade HCl (UpA Romil) to pH1.9 (~0.013 mol H^+ L^{-1}). Samples from D361 were analyzed using a flow injection analysis system equipped with a Toyopearl AF-Chelate-M650 (Tosch) resin via luminol chemiluminescence [*Klunder et al.*, 2011]. Surface seawater samples collected during AMT21 were analyzed for Fe by off-line isotope dilution inductively coupled plasma–mass spectrometry (Element XR, Thermo), following previously outlined methods [*Milne et al.*, 2010]. The accuracy of previously unreported AMT21 data was assessed by the determination of Fe in seawater reference materials (Sampling and Analysis of Fe (SAFe) and GEOTRACES). The standard seawaters were in good agreement with the reported consensus values (GD = 0.940 nmol L^{-1} (1.00 nmol L^{-1}), SAFe S = 0.095 nmol L^{-1} (0.093 nmol L^{-1}), and SAFe D2 = 0.933 nmol L^{-1} (0.933 nmol L^{-1})).

2.3. The pCO_2 and SST

Near-surface temperature (~2 m, henceforth assumed to be SST) was measured throughout all seven cruises using a vessel mounted Sea-Bird 38 or similar temperature sensor. For cruises, AMT21, AMT17, D326, M55, and M60, direct measurement of pCO_2 were conducted as described in *Hardman-Mountford et al.* [2008], *Kitidis et al.* [2012], and *Körtzinger* [1999]. During D361 and JC32, dissolved inorganic carbon (DIC) and total alkalinity (TA) was sampled from near-surface fired Ocean Test Equipment (OTE) bottles. DIC analysis was performed using the standard coulometric technique, while TA was analyzed using standard titrimetric techniques [*Dickson et al.*, 2007]. The partial pressure of CO_2 was derived from these parameters following equations outlined in *Dickson et al.* [2007].

2.4. *Trichodesmium* sp. Abundance

Trichodesmium abundance was measured during AMT17, JC32, D326, D361, and AMT21. Entire 20 L OTE bottles fired near the surface (~2 m) were gravity filtered through membranes or polycarbonate filters (Millpore Isopore; 10 μm pore size, 47 mm diameter). Colonies and free trichomes were gently agitated to remove them from the surface of the membrane or filter before being preserved in 2% Lugol's iodide and stored in the dark. Filters were visually inspected for complete resuspension of *Trichodesmium* colonies and free trichomes. Colony and free trichome abundance, colony morphology, and approximate colony size were enumerated using light microscopy. The limit of detection for *Trichodesmium* abundance was equivalent to 0.05 Trichomes L^{-1}.

2.5. N_2 Fixation Rates

Whole community N_2 fixation rates were measured during M55, M60, AMT17, JC32, D326, D361, and AMT21 following the method described by *Montoya et al.* [1996]. Briefly, 4.5 L (AMT17, D326, D361 JC32, and AMT21) or 1.2 L (M55 and M60) polycarbonate bottles (Nalgene) were filled, ensuring that no air bubbles remained and sealed with silicone septa containing screw caps. Each bottle was spiked with 4 mL (AMT17, D326, D361 JC32, and AMT21) or 1 mL (M55 and M60) $^{15}N_2$ gas (99%, Campro or Cambridge Scientific, see below) and incubated for 24 h at sea surface temperature (SST) and near-sea surface irradiance achieved using on deck incubators cooled using the ship's underway seawater supply system and shaded using optical filters (0.15 neutral density). Following incubation samples were filtered onto preashed glass fiber filters (450°C for 12 h, Whatman GF/F or Fisherbrand MF300), folded into 1.5 mL tubes (Eppendorf), and dried for 24 h at 40°C. Upon return to the laboratory, filters were encapsulated in a tin disk and analyzed for organic nitrogen and $^{15}N/^{14}N$ ratio using elemental analyzer isotope ratio mass spectrometry.

Trichodesmium specific N_2 fixation rates were also measured during both D361 and AMT21. Colonies were collected at dawn using plankton net tows. Fifty colonies were then isolated using plastic inoculation loops and placed into 125 mL polycarbonate bottles (Nalgene) filled with 0.22 μm filtered trace metal clean surface water. Bottles were filled entirely, sealed with silicone septa containing screw caps, and spiked with 0.5 mL $^{15}N_2$. Bottles were incubated for 12 h at SST and sea surface irradiance before being filtered onto preashed GF/F filters, dried, and stored until analysis according to the method described for the whole community.

Recent work has highlighted potential contamination issues with commercial $^{15}N_2$ gas stocks [*Dabundo et al.*, 2014]. The stocks used during the reported cruises were purchased from Campro Scientific (M55 and M60, lot

numbers not recorded) and Cambridge Isotopes (AMT17, D326-lot # I1-8518; JC32, D361, AMT21-lot # I1-11785A). Although these stocks are either known (Cambridge Isotopes lot # I1-11785A) or were likely to be relatively clean [*Dabundo et al.*, 2014], using a similar calculation to *Dabundo et al.* [2014], we estimated a potential upper bound for apparent N_2 fixation due to contaminants (i.e., an effective detection limit) of ~0.05 nmol N L^{-1} d^{-1}. Additionally a systematic approximately twofold underestimation of the absolute N_2 fixation rates is likely to have influenced the absolute rates derived due to incomplete equilibration of the N_2 gas over the experimental time scale [*Mohr et al.*, 2010; *Großkopf et al.*, 2012; *Wilson et al.*, 2012]. However, given that observed community rates and *Trichodesmium* specific rates spanned >2 and >3 orders of magnitude, respectively, neither background apparent rates due to gas contamination or systematic underestimation are likely to have any significant bearing on our conclusions, which are based on the observed interrelationship between variables within the data set.

2.6. Numerical Model

To support our observations and the conceptual resource ratio framework used for interpreting the nutrient-diazotroph interrelationships, we used a previously employed numerical box model [*Tyrrell*, 1999; *Dutkiewicz et al.*, 2012; *Ward et al.*, 2013; *Schlosser et al.*, 2014]. The differential equations describing the evolution of state variables were effectively identical to those detailed in *Ward et al.* [2013] and *Schlosser et al.* [2014], with parameters, model equations, and initial conditions as described in the latter. Briefly, the model is integrated in a series of linked boxes taken to represent the "surface" and "thermocline" regions of the water column. Three nutrients (N, P, and Fe) interact with diazotrophs and nondiazotrophs in the surface boxes, while organic material transported to the thermocline box is simply remineralized back to dissolved nutrients [*Schlosser et al.*, 2014]. The model was further expanded to include two distinct diazotrophs (D1 and D2), with D1 parameterized as in *Schlosser et al.* [2014], while D2 was ascribed a 20% elevated P requirement alongside a 20% reduction in Fe requirement, making it a better competitor for P but a poorer competitor for Fe. The only external forcing provided is a variable source of DFe to one or more of the surface boxes, which was originally taken to represent differing atmospheric Fe input scenarios [*Schlosser et al.*, 2014], although this could be equally applicable to any other Fe sources including, for example, riverine or sedimentary inputs. For the current study, iron input was arbitrarily represented by a Gaussian distribution with a half width of four surface boxes and peak inputs that were varied over a twentyfold range between 28 runs.

3. Results and Discussion

Sea surface temperatures ranged from 19.6 to 28.7°C, with a single station (JC32) located in the upwelling region to the west of Africa having a lower temperature of 16.4°C (23.7°S, 13.7°E). Excepting this station, all observed temperatures were within previously published temperature tolerances (18–32°C) for a range of *Trichodesmium* culture strains [*LaRoche and Breitbarth*, 2005; *Breitbarth et al.*, 2007; *Fu et al.*, 2014] and temperature ranges observed to be associated with other groups [*Moisander et al.*, 2010]. Observed variability in pCO_2 across the sampled region was modest (332–464 μatm), with absolute values typically higher than half saturation constants ($K_{1/2}$) for N_2 fixation as a function of pCO_2 for the majority of studied *Trichodesmium* culture strains [*Hutchins et al.*, 2013].

The location of the ITCZ is affected by sea surface temperature (SST), and as such, the ITCZ shows an asymmetrical seasonal migration [*Mitchell and Wallace*, 1992] which influences the position of the biogeochemical transition region between the northern and southern oligotrophic regions of the Atlantic [*Schlosser et al.*, 2014]. The seasonal synchronicity between precipitation and DFe distributions in the (sub)tropical Atlantic as described in *Schlosser et al.* [2014] is further supported in the current study with the inclusions of the previously unpublished N_2 fixation data from AMT21 (Figure 2e). The region of maximal precipitation used here to represent the location of the ITCZ was observed between 4°N and 8°S during D361, while for AMT21 and AMT17, the maximum precipitation was observed farther north between 11.5°N–2°N and 10.5°N–4°S, respectively (Figure 2). The ITCZ is at its northern and southernmost position in July and January, respectively [*Philander et al.*, 1996; *Xie and Saito*, 2001]. Given that the dates of D361 and AMT21/AMT17 are midphase in relation to this seasonality, it is likely that there is a greater latitudinal migration than what our observations indicate.

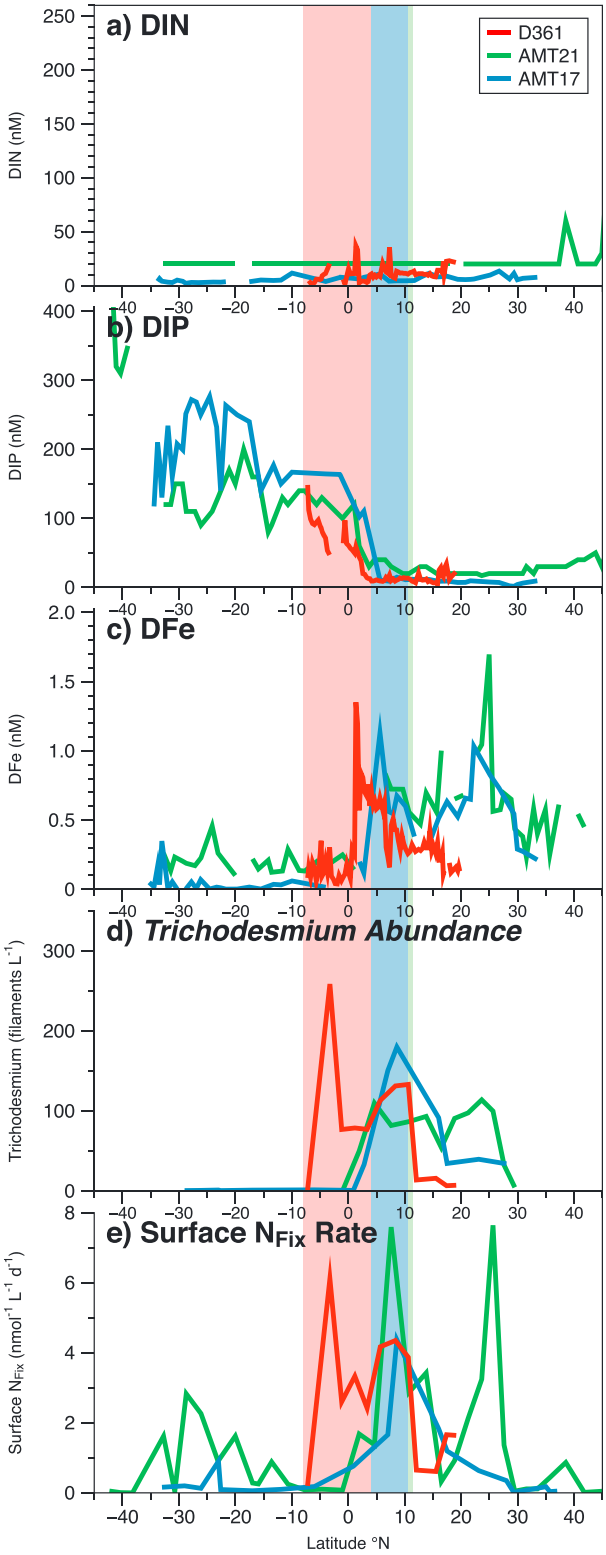

Figure 2. Previously unpublished data collected along an Atlantic Meridional Transect (AMT21, green) at ~25°W during northern hemisphere spring and autumn compared with two previous cruises, AMT17 (blue) and D361 (red). (a) Dissolved inorganic nitrogen, DIN (nM). (b) Dissolved inorganic phosphorus, DIP (nM). (c) Dissolved iron, DFe (nM). (d) *Trichodesmium* abundance (Trichomes L^{-1}). (e) Whole community surface N_2 fixation rates (nmol L^{-1} d^{-1}). The shaded regions represent enhanced surface rainfall as defined by precipitation $>2 \times 10^{-5}$ kg m^{-2} s^{-1} as derived from NCEP reanalysis daily average surface flux data. The enhanced precipitation region indicated the approximate location of the ITCZ during AMT17 (15 October to 28 November 2005, blue), D361 (7 February to 19 March 2011, red), and AMT21 (29 September to 14 November 2011, green).

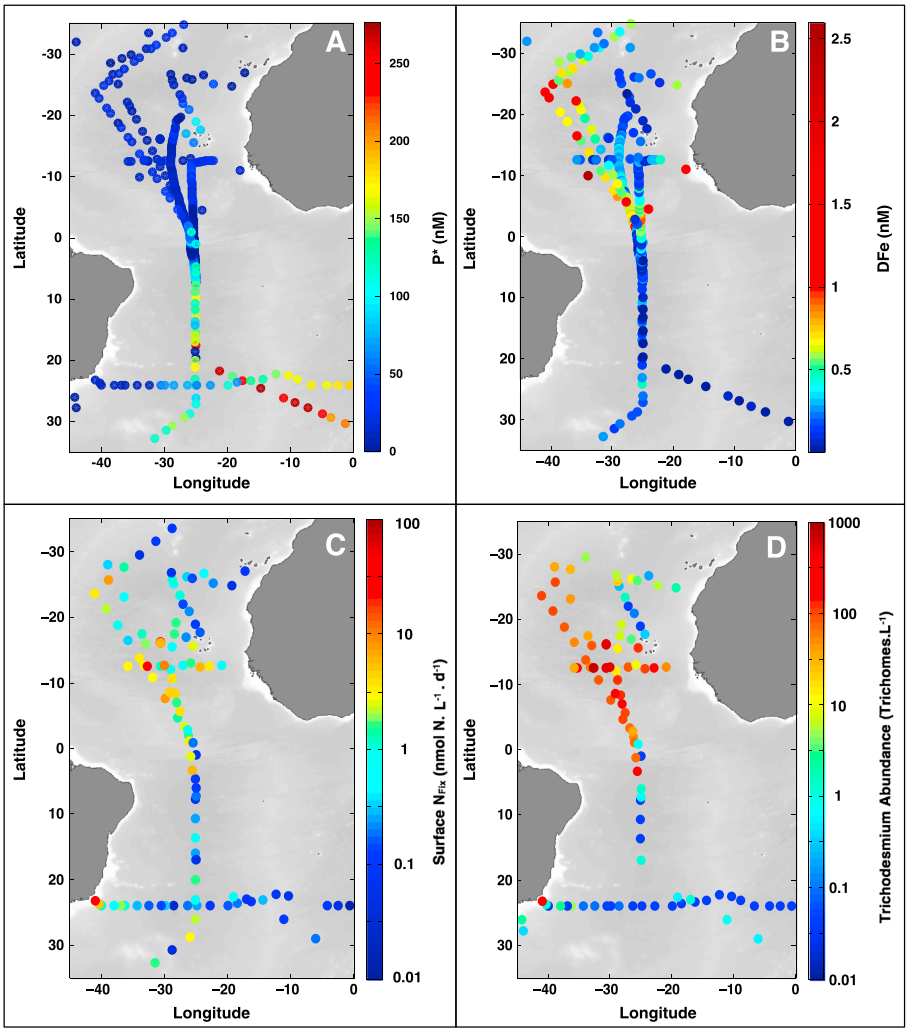

Figure 3. Data collected from cruises M55 (October to November 2002, R/V *Meteor*), M60 (November to December 2003, R/V *Meteor*), AMT17 (Octpber to November 2005, RRS *Discovery*), D326 (January to February 2008, RRS *James Cook*), JC32 (March to May 2009, RRS *James Cook*), D361 (February to March 2011, RRS *Discovery*), and AMT21 (October to November 2011, RRS *Discovery*). (a) P* (nM) = DIP − DIN/$r_{n/p}$. (b) Dissolved iron, DFe (nM). (c) Whole community surface N_2 fixation (nmol L^{-1} d^{-1}). (d) *Trichodesmium* abundance (trichomes L^{-1}).

Surface DIN concentrations remained consistently low throughout the sampled regions, with a mean concentration of 12 ± 10 nM (mean ± SD, $n = 276$) (Figures 2a, 4a, 4e, and 4i). The NASG consistently displayed greatly diminished DIP concentrations when compared with the SASG (22 ± 19 nM ($n = 126$) and 126 ± 60 nM ($n = 197$), respectively) (Figures 2b, 3a, 4b, 4f, and 4j). Conversely the distribution of DFe revealed consistently elevated concentrations in the Saharan dust-influenced NASG (0.42 ± 0.33 nM, $n = 189$) when compared with the SASG (0.13 ± 0.11 nM, $n = 107$), where little dust deposition is evident [*Jickells*, 2006] (Figures 2c and 3b). The new measurements from the AMT21 cruise presented here were consistent with prior analysis based on the D361 and AMT17 cruises [*Schlosser et al.*, 2014], suggesting that observed north-south migration of DIP and DFe gradients is associated with the seasonal migration of the ITCZ [*Schlosser et al.*, 2014]. Specifically, AMT 21 and 17 showed elevated DFe concentrations in the central NASG around 20°N–5°N, while D361 (red) shows this band of high DFe shifted south between 5°N and 0°N (Figures 2c and 3b).

Trichodesmium colonies and free trichomes were observed during all seven cruises. Near-surface *Trichodesmium* abundance was densest in the southern region of the NASG and seasonally associated with the ITCZ-influenced region (~15°N–7°S) (Figures 2d and 3d), consistent with previous observations [*Capone et al.*, 2005; *Fernandez et al.*, 2010; *Sohm et al.*, 2011b; *Luo et al.*, 2012; *Schlosser et al.*, 2014]. Observations

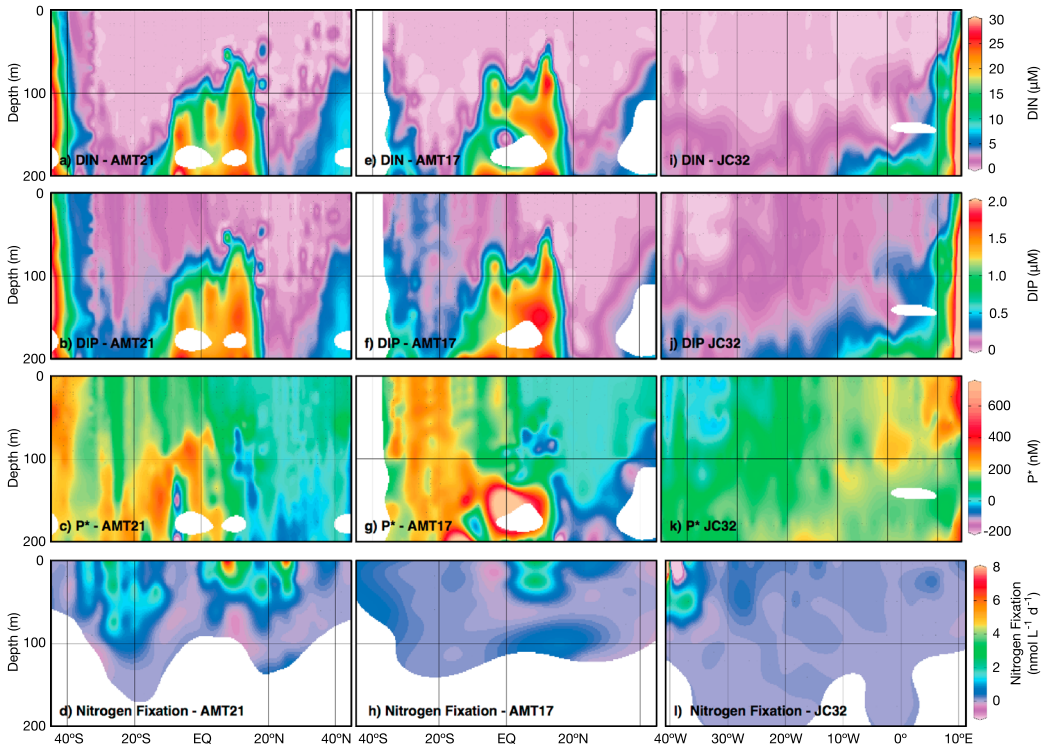

Figure 4. Contour plots presenting DIN (nM), DIP (nM), P* (nM), and N_2 fixation rates (nmol L^{-1} d^{-1}) within the euphotic zone for (a–d) AMT21, (e–h) AMT17, and (i–l) JC32, with data from AMT21 and JC32 being previously unpublished. Cruise JC32 crossed the AMT21 transect at ~25°W, crossed AMT17 at ~17.25°W. AMT17 and AMT21 both cross the JC32 transect at ~24°S–25°S.

from AMT21 and AMT17 revealed *Trichodesmium* to be consistently abundant throughout the sampled regions of the NASG (mean ± SD, 76 ± 33, and ~70 ± 64 trichomes L^{-1}, respectively) before sharply declining to undetectable concentrations south of ~0°N. The observed population density maximum during D361 was located farther south, with *Trichodesmium* observed between 19°N and ~7°S (82 ± 72 trichomes L^{-1}) (Figure 2d). Consistent with previous observations [*Moore et al.*, 2009; *Sohm et al.*, 2011a], *Trichodesmium* was not observed in the central SASG during any of these cruises. In contrast, during the JC32 cruise, significant *Trichodesmium* populations and associated community N_2 fixation rates were observed within the core of the Brazil current, adjacent to the continental shelf on the far western edge of the SASG. On-shelf blooms of *Trichodesmium* have also been reported in this region [*Carvalho et al.*, 2008]. Moreover, enhanced rates of community N_2 fixation were directly observed in the upper water column during the north-southwest crossing of the western side of the SASG during AMT21 (Figure 4d).

Surface community N_2 fixation rates observed across large regions of the Atlantic correlated well with *Trichodesmium* biomass ($r = 0.72$, $P < 0.05$) particularly over the range of higher N_2 fixation rates and *Trichodesmium* abundances (Figure 5). At lower *Trichodesmium* abundance, the observed relationship decouples, likely representing an increased contribution of the non-*Trichodesmium* diazotrophic community to measured whole-community N_2 fixation rates, potentially alongside any contribution by trace level contaminants in $^{15}N_2$ gas [*Dabundo et al.*, 2014]. Mean *Trichodesmium* specific N_2 fixation rates assessed during both D361 and AMT21 ($n = 24$) supported the inferred increased contribution of the non-*Trichodesmium* diazotrophic community at lower N_2 fixation rates, although any potential for differential underestimation of N_2 fixation rates between diazotrophic groups [*Großkopf et al.*, 2012] could weaken such inferences. Acknowledging such caveats, elevated whole community N_2 fixation appeared a strong indicator of *Trichodesmium* specific N_2 fixation, in agreement with previous work [*Fernandez et al.*, 2010] in the tropical Atlantic, where observed N_2 fixation rates closely matched predicted N_2 fixation rates derived from *Trichodesmium* abundance.

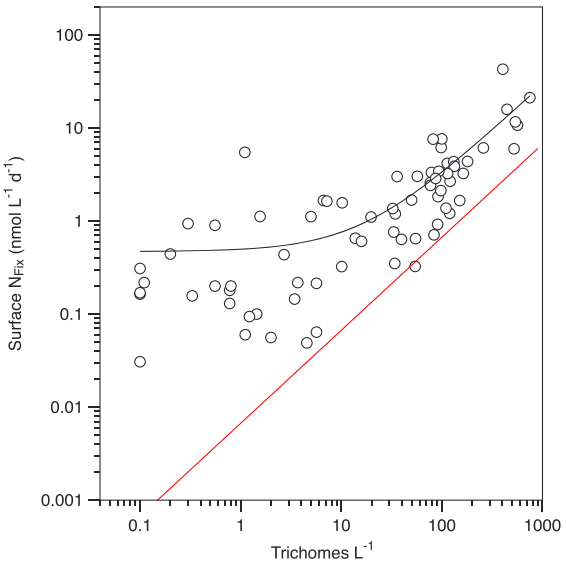

Figure 5. Correlation between *Trichodesmium* abundance (trichomes L^{-1}) and whole community N_2 fixation rates (nmol L^{-1} d^{-1}) shown in black, $R^2 = 0.86$. The measured mean N_2 fixation per trichome (nmol N trichome^{-1} d^{-1}) is shown in red.

Surface community N_2 fixation rates showed a similar north-south divide as observed in *Trichodesmium* abundance, with the bulk of diazotrophic activity observed in the southern flanks of the NASG and the equatorial region (Figures 3c, 6a, and 6b) consistent with previous observations [*Luo et al.*, 2012]. Within the boundary between the NASG and SASG, a strong seasonality is observed between spring (D361, red) and autumn (AMT17, blue and AMT21, green) cruises where peak surface N_2 fixation rates follow the pattern of DFe and reside farther south during D361 when compared with either AMT cruise (Figure 2) as previously indicated [*Schlosser et al.*, 2014].

3.1. Simple Linear Regression Analysis

Relationships between environmental and diazotroph-related variables were initially investigated using simple linear regression analysis as in *Luo et al.* [2013]. A weak ($R^2 < 0.07$) yet significant negative correlation was observed between surface N_2 fixation and DIP (Figure 7c and Table 1). No other significant correlation was found between SST, pCO_2, DIP, or DFe and *Trichodesmium* abundance or SST, pCO_2, or DFe and surface N_2 fixation rates (Figure 7 and Table 1). Variations in these four environmental variables, all of which have been proposed as potential controls on diazotrophy, were thus of limited predictive value for measured community N_2 fixation rates or *Trichodesmium* biogeography across the observed environmental ranges in the (sub)tropical Atlantic (Figure 7).

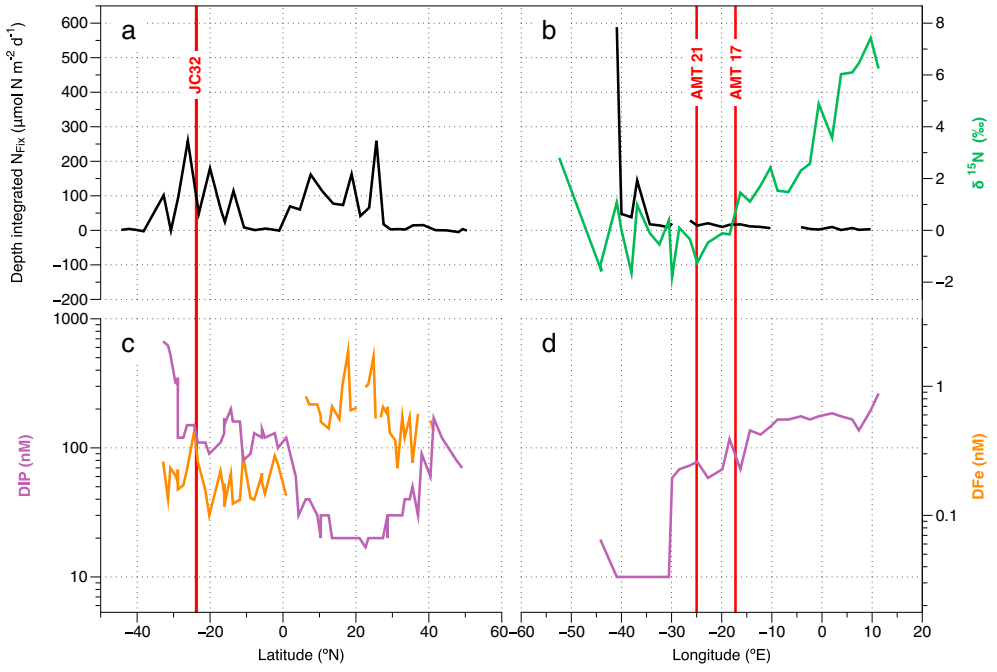

Figure 6. Depth-integrated N_2 fixation rates and δ^{15}PON natural abundance data observed during (a) AMT21 (N_2 fixation only) and (b) JC32. DFe (orange) and DIP (purple) surface water concentrations observed during (c) AMT21 and (d) JC32 (DIP only).

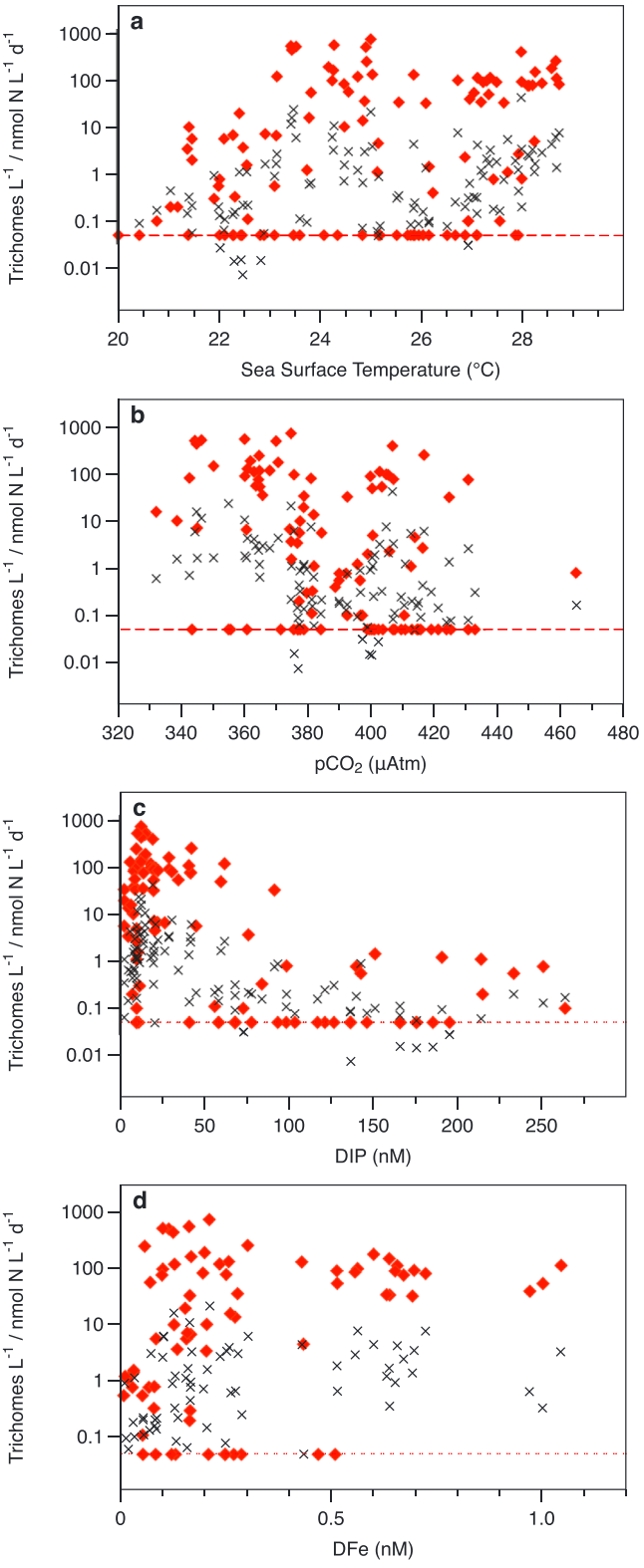

Figure 7. *Trichodesmium* abundance (trichomes L^{-1}) (red diamonds) and whole community N_2 fixation rates (nmol L^{-1} d^{-1}) (black crosses) as a function of observed (a) SST (°C), (b) pCO_2 (µatm), (c) DIP (nM), or (d) DFe (nM).

As noted above, the sampled range for SST was within the temperature tolerance range of studied *Trichodesmium* isolates [*Fu et al.*, 2014]. Moreover, the current analysis contrasts with the findings of *Luo et al.* [2013] who observed a significant correlation between temperature and N_2 fixation across a broader temperature and geographical range. Overall, it is clearly difficult to establish any strong inference from correlative studies of this type. Thus, it remains unclear whether large-scale correlations of SST and *Trichodesmium* populations provide evidence for the importance of a direct physiological driver [*Fu et al.*, 2014] or result from stronger control by covarying factors such as low N environments and increased stratification, with temperature optima then being a secondary adaptation [*LaRoche and Breitbarth*, 2005; *Ward et al.*, 2013]. Irrespectively, within the sampled range, any direct temperature-related ecophysiological effect [*Fu et al.*, 2014] appears to be overridden by other drivers.

On the basis of the performed correlation analysis, the marked coherent order of magnitude variability we observed in overall diazotrophy and *Trichodesmium* abundance also appeared to be unrelated to any direct physiological pCO_2 driver. Although observed pCO_2 values in the sampled region were typically higher than most measured *Trichodesmium* $K_{1/2,pCO2}$ (Figure 7b), some currently studied strains have higher values [*Hutchins et al.*, 2013]. Thus, the potential for pCO_2 to have a selective influence between *Trichodesmium* ecotypes can certainly not be excluded on the basis of our observations, but once again, any effect on the overall biogeography of *Trichodesmium* or the bulk diazotroph community appeared to be overridden, or at least masked, by other factors.

Table 1. Coefficients of Determination[a]

Parameter	Community N_2 Fixation	Trichodesmium Abundance
SST	0.03 ($n = 107$)	0.01 ($n = 79$)
pCO_2	0.02 ($n = 95$)	0.09 ($n = 70$)
DFe	0.04 ($n = 69$)	0.00 ($n = 62$)
DIP	**0.06 ($n = 105$)**	0.07 ($n = 74$)

[a]Coefficient of determination (R^2) for either community N_2 fixation or *Trichodesmium* abundance compared with SST, pCO_2, DFe, and DIP in paired samples. Sample size is shown in brackets, significant correlation as determined by Student's *t* test ($P < 0.01$) are highlighted in bold font.

The absence of predictive capability for DIP and DFe as individual variables contrasts with a prior analysis based on a subset of these data [*Moore et al.*, 2009] but is more consistent with the broader study of *Luo et al.* [2013]. However, unlike SST and pCO_2, which will not be directly influenced by the activity of diazotrophs, or in the case of pCO_2 only weakly influenced at most [*Foster et al.*, 2007; *Subramaniam et al.*, 2008], reciprocal feedback between microbial processes and any nutrients potentially limiting these processes are expected to be strong, to the point of potentially being dominant controls [*Tilman*, 1980; *Cullen*, 1991; *Ward et al.*, 2013]. The lack of a direct correlation between a limiting nutrient and organism biogeography or activity would be fully expected under many circumstances [*Cullen*, 1991] and certainly cannot provide unequivocal evidence for the absence of a relationship. Indeed, if it is assumed that both DIP and DFe are essential nutrients in the sense of *Tilman* [1980], with diazotrophs in general and *Trichodesmium* in particular requiring both for growth, relationships between both these nutrients and N_2 fixation and/or *Trichodesmium* abundance must all be considered together within a theoretical framework capable of explaining observations [*Dutkiewicz et al.*, 2012; *Ward et al.*, 2013; *Dutkiewicz et al.*, 2014].

3.2. Resource-Ratio Theory

Resource competition theory dictates that the organism best able to utilize a given resource will deplete that resource down to a well-defined minimum concentration, termed the R^* value [*Tilman*, 1980]. At steady state, this framework supports a niche for as many competing species as there are different potential limiting resources. Temporarily considering nutrients as the sole potential limiting resource, the abundance and activity of the diazotrophic community are expected to be controlled by the relative supply rates of N, P, and Fe [*Ward et al.*, 2013]. Diazotrophs such as *Trichodesmium* will avoid competitive exclusion by nondiazotrophs in regions where the nondiazotrophic community is N limited [*Monteiro et al.*, 2011; *Dutkiewicz et al.*, 2012; *Ward et al.*, 2013]. Such steady state N limitation of nondiazotrophs is likely a reasonable approximation for the sampled regions of the (sub)tropical Atlantic [*Moore et al.*, 2013], consistent with the observed uniform low (<20 nM) DIN concentrations (Figure 2a) and multiple experimental studies [*Ryther and Dunstan*, 1971; *Graziano et al.*, 1996; *Mills et al.*, 2004; *Moore et al.*, 2009].

Adopting the simplest assumption, where diazotrophs consume Fe and P at a fixed ratio, as net growth proceeds from a starting condition, both nutrients would be expected to be removed along a fixed consumption vector (Figure 8a) until one is depleted to the R^* concentration [*Ward et al.*, 2013]. Once a nutrient has been depleted to R^*, equilibrium uptake is balanced by supply, and zero net growth is achievable. Under this condition, the biomass of the stable diazotroph population will then be proportional to the (re)supply of the limiting nutrient divided by the mortality rate [*Dutkiewicz et al.*, 2009, 2012]; i.e., the diazotroph standing stock and overall diazotrophy are not expected to be related to the steady state concentration of the limiting nutrient. Consequently, over a sufficiently large range of Fe or P supply ratios, the interaction between diazotrophic growth and Fe and P availability is expected to result in a characteristic "L-shaped" relationship between the residual Fe and P concentrations at equilibrium (Figure 8a). The corner of the "L," which represents the optimal Fe:P supply ratio, defines the transition between either Fe or P limitation, with populations of diazotrophs located along the R^*_{Fe} isocline being Fe limited, while populations along the R^*_P isocline are P limited (as illustrated in Figure 8a).

Such conceptual arguments can be illustrated using simple numerical models of the system [*Dutkiewicz et al.*, 2012; *Ward et al.*, 2013; *Schlosser et al.*, 2014]. Crucially, the magnitude of the equilibrium diazotroph biomass is expected to depend on the absolute supply rates of the limiting nutrient and mortality [*Dutkiewicz et al.*, 2012; *Ward et al.*, 2013], while the nutrient limitation status is entirely dictated by the supply ratios of different nutrients compared to biological requirements [*Ward et al.*, 2013]. Thus, even within a simple illustrative numerical model, where the activity and abundance of diazotrophs is entirely controlled by

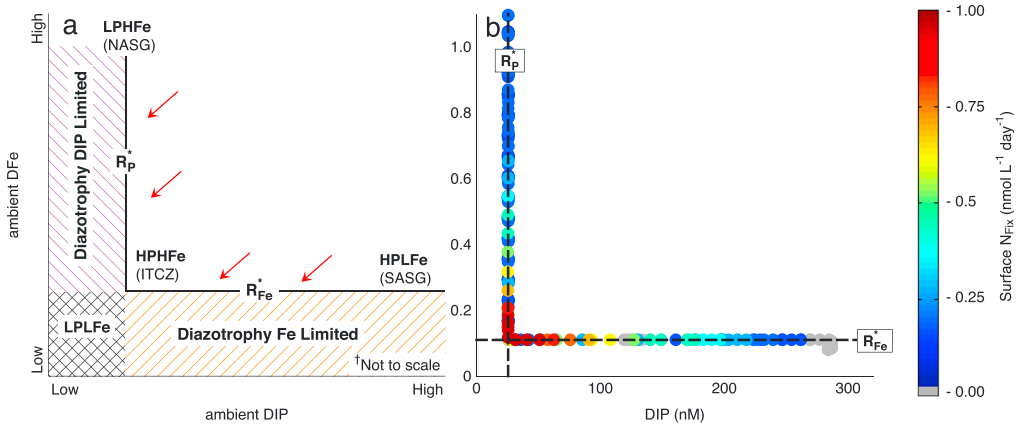

Figure 8. (a) Graphical representation of the resource competition theory conceptual framework. The red arrows indicate nutrient consumption vectors. (b) Numerical model output showing surface N_2 fixation rates (nmol L^{-1} d^{-1}) as a combined function of DIP (nM) and DFe (nM) for a range of different model realizations.

parameterized nutrient limitation, there is no simple equilibrium relationship between diazotrophic activity or biomass and the concentration of either nutrient (Figure 8b), emphasizing how observed concentrations of limiting nutrients are expected to be a consequence of microbe-nutrient interactions [*Cullen*, 1991; *Ward et al.*, 2013]. In contrast, within the current context, a robust, repeatable characteristic L-shaped relationship between two limiting nutrients, P and Fe, emerges as a result of diazotrophic activity (Figure 8b). The arms of the L reflect the so-called zero-net growth isoclines [*Tilman et al.*, 1982] corresponding to the *R** values for the respective nutrients (Figure 8), which in the simplest case are given by [*Tilman*, 1980; *Dutkiewicz et al.*, 2012; *Ward et al.*, 2013]:

$$R^*_{Fe} = \frac{k_{Fe}}{\frac{\mu_{max}}{m} - 1} \quad (1)$$

$$R^*_{P} = \frac{k_{P}}{\frac{\mu_{max}}{m} - 1} \quad (2)$$

where k_{Fe} and k_P represent the half saturation coefficients for growth on Fe and P, respectively, and μ_{max} and m are the maximum growth rate and total mortality rate, respectively.

Within the adopted framework for the model [*Schlosser et al.*, 2014], peak diazotroph biomass within a single realization occurs strictly at the apex of the L. However, performing multiple runs, for example, varying the magnitude of peak Fe input can reveal more complex emergent patterns of diazotrophy. Although there is a tendency for the highest biomass to typically occur around the low Fe-low P transition region (Figure 8b), high rates can actually be found along the arms of the L as, to reiterate again, biomass and activity are a function of both limiting nutrient supply rate and mortality, while the equilibrium limiting nutrient concentration is independent of supply [*Dutkiewicz et al.*, 2009, 2012; *Ward et al.*, 2013].

Comparing our compiled data set with these simple conceptual and numerical models (Figures 8a and 8b), we observed a characteristic L-shaped relationship between residual surface DIP and DFe concentrations in the sampled regions of the oligotrophic Atlantic Ocean (Figures 9a and 9c). Moreover, despite less data being available, a similar relationship was observed between TDP and DFe (Figures 9b and 9d). Similarly, incorporation of a range of treatments of DOP and dissolved organic nitrogen cycling within the model framework (not shown) introduced no qualitative difference in the emergent relationships between DFe and DIP* and TDP* compared to the simplest case (Figure 8).

Community N_2 fixation and *Trichodesmium* abundance both displayed a tendency toward maximal values in regions observed to be deplete in both DFe and DIP (TDP), i.e., generally associated with the transition between regions of higher residual DFe and DIP (Figure 9). We thus suggest that recognition of the potential for diazotrophic activity to drive depletion of DIP (TDP) and/or DFe, as would be predicted from the theory of *Ward et al.* [2013] and occurs within the simple model (Figure 8), in keeping with more complex realizations [*Monteiro et al.*, 2011; *Dutkiewicz et al.*, 2014], is crucial for interpreting observed

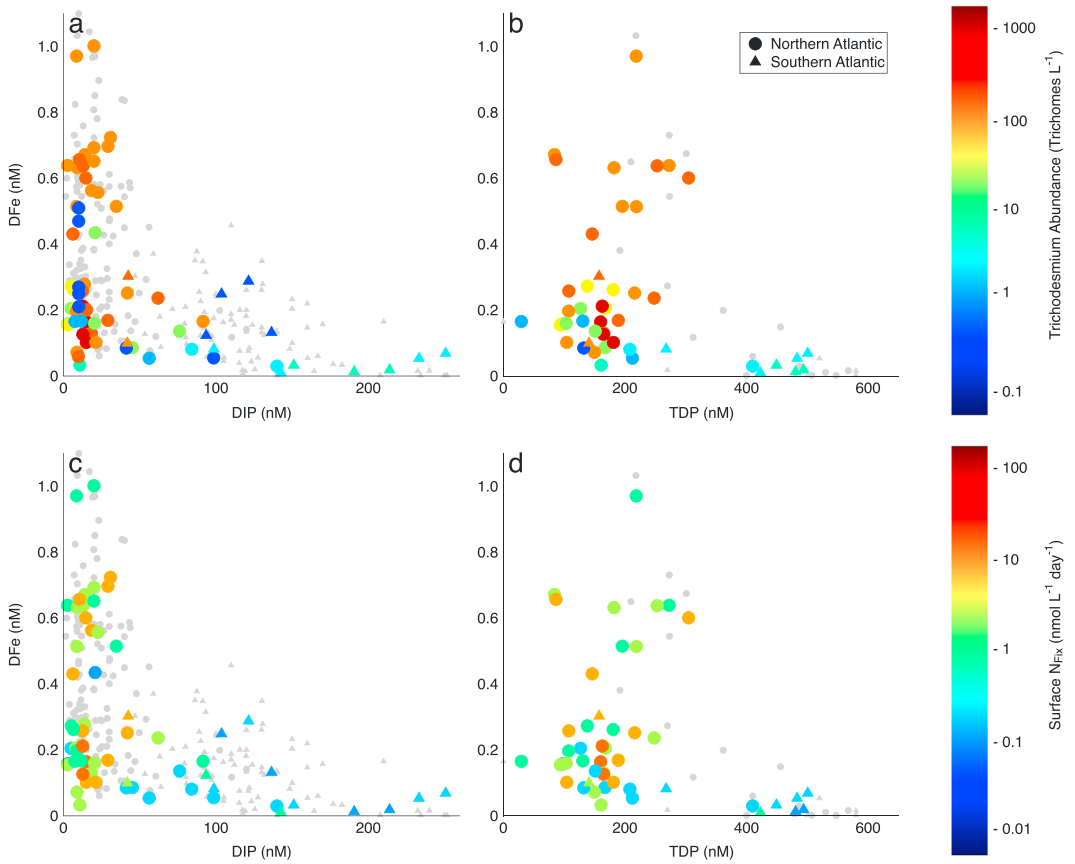

Figure 9. Relationship between DIP (nM) and DFe (nM) across the complete data set including stations where no measurements of either *Trichodesmium* abundance or net community N_2 fixation rates were available (grey symbols). (a and b) *Trichodesmium* abundance (trichomes L^{-1}) as a function of DFe (nM) and either (Figure 9a) DIP or (Figure 9b) TDP (nM). (c and d) Surface N_2 fixation rates (nmol L^{-1} d^{-1}) as a function of DFe (nM) and either (Figure 9c) DIP or (Figure 9d) TDP (nM). The circles denote observations taken from the northern hemisphere, while the triangles denote observations from the southern hemisphere.

relationships between diazotrophs and these potentially limiting nutrients in the ocean (Figures 7 and 10). Recent evidence has also suggested that diazotrophs may have a preference for simultaneous DFe and DIP deplete regions [*Garcia et al.*, 2015]. However, it is not clear how such behavior would influence the large-scale patterns between DFe and DIP observed in the Atlantic (Figure 9).

The observed L-shaped relationship between DIP and DFe is thus argued to be both a result of and diagnostic of large-scale controls and feedback between limiting nutrients and diazotrophy over our sampled region, with ambient DFe and DIP concentrations residing at, or close to, their R^* concentrations, while overall community N_2 fixation rates and/or the standing stock of *Trichodesmium* are then a function of the Fe or P supply rate, rather than the concentrations of these nutrients. The conformity of our environmental observations to the theoretical expectations strongly supports an argument for persistent contrasting regions of Fe and P limitation [*Moore et al.*, 2009; *Sohm et al.*, 2011b] characterizing the sampled region of the Atlantic ocean, while at the same time questioning the proximal importance of other proposed drivers such as SST and pCO_2 [*Breitbarth et al.*, 2007; *Hutchins et al.*, 2013], at least within the (sub)tropical Atlantic Ocean.

3.3. Diazotrophy in the Western SASG

In addition to the *Trichodesmium*-attributed diazotrophic activity of the NASG and equatorial Atlantic, our observations revealed significant rates of N_2 fixation in the western SASG (Figures 3c and 4d). The SASG is grossly undersampled with regards to N_2 fixation rates, with few published data, the majority being surface water only [*Luo et al.*, 2012]. Comparing the NASG and SASG along the AMT21 transect which sampled the western side of the gyre, we calculated near-equivalent average depth integrated rates between the two gyres with 55 and 53 umol N m^{-2} d^{-1} fixed in the NASG and SASG leg of this transect,

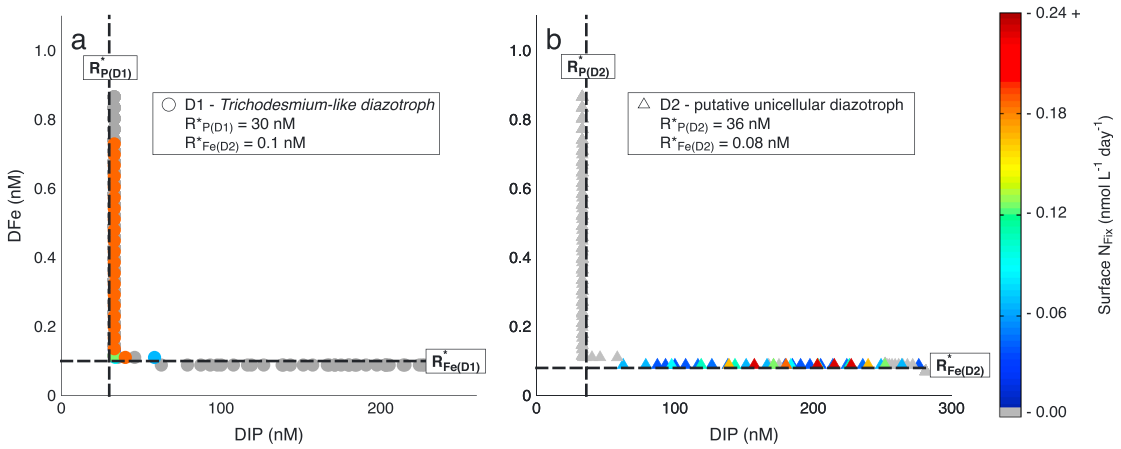

Figure 10. Model output showing surface N_2 fixation rates (nmol L^{-1} d^{-1}) as a function of DIP (nM) and DFe (nM) for two theoretical diazotrophs, D1 a *Trichodesmium*-like diazotroph best at competing for (a) P and D2 a putative-unicellular diazotroph best at competing for (b) Fe.

respectively (Figure 6a). Similarly, depth-integrated rates during the JC32 west-east transect across the gyre peaked near to the western margin in a region of depleted DIP, low surface P*, and low $\delta^{15}N$ approaching 0‰ (Figures 6b and 6d). The latter is also consistent with an increased importance for N_2 fixation [*Montoya et al.*, 2004; *Mahaffey et al.*, 2005] in the western SASG as opposed to the eastern basin. Recent observations of H_2 supersaturation are also suggestive of a significant diazotrophic community in the western portion of the SASG basin [*Moore et al.*, 2014] and are consistent with our new direct and likely underestimated [*Mohr et al.*, 2010; *Großkopf et al.*, 2012; *Wilson et al.*, 2012] observations of significant N_2 fixation region.

As has been previously observed [*Carpenter et al.*, 2004; *Capone et al.*, 2005], highest rates of diazotrophy in the NASG are typically observed in near-surface waters (Figure 4d). In contrast, our observation of SASG diazotrophy indicated a more homogeneous distribution throughout the entire euphotic zone (Figure 4d). Unicellular diazotrophs often appear to be more homogeneously distributed throughout the euphotic zone when compared with *Trichodesmium* [*Montoya et al.*, 2004], which can tend to aggregate in surface waters, but has rarely been observed in the SASG [*Tyrrell et al.*, 2003; *Moore et al.*, 2009; *Fernandez et al.*, 2010; *Goebel et al.*, 2010]. We thus suggest that emerging consistent evidence of significant diazotrophic activity in the western SASG is potentially associated with unicellular diazotrophs, which may be heterotrophic or cyanobacterial in origin and irrespectively might be expected to have different nutrient affinities or growth strategies.

In contrast to the NASG, where high rates of *Trichodesmium* associated N_2 fixation have a tendency to be distributed along the R^*_P "arm" of the L-shaped DFe-P relationship (Figure 9a), the SASG diazotrophic community is associated with the R^*_{Fe} arm, where DFe concentrations are low (Figure 9a). Higher Fe requirements for *Trichodesmium* as a result of near concurrent N_2 fixation and photosynthetic activity [*Berman-Frank et al.*, 2001] might be expected to result in competitive exclusion by any hypothesized unicellular diazotrophic community under conditions which are Fe limiting for diazotrophy [*Monteiro et al.*, 2010]. For example, the unicellular diazotroph *Crocospheara watsonii* employs a mechanism of iron "hot bunking," whereby temporal segregation of N_2 fixation and photosynthesis allows for an intracellular recycling of metalloprotein bound iron [*Saito et al.*, 2011], thus reducing the effective R^*_{Fe}. Such an iron conservation strategy is unlikely in *Trichodesmium* given the substantially shorter time period between peak N_2 fixation and photosynthesis [*Berman-Frank et al.*, 2001].

Dominance of *Trichodesmium* within the "high Fe-low P" NASG but not the "lower Fe-higher P" SASG could thus be interpreted as indicating that *Trichodesmium* spp. are the best diazotrophic competitors for P (i.e., have a lower R^*_P). *Trichodesmium* spp. appear to have a number of novel P compensatory adaptations, including the potential for uptake of a wide range of DOP compounds [*Dyhrman et al.*, 2006; *Orchard et al.*, 2009, 2010], which is broadly consistent with observed depletion of DOP in the NASG [*Moore et al.*, 2009]. Indeed, organisms access the phosphomonoester proportion of the DOP pool using the exoenzyme alkaline phosphatase, with the activity of these enzymes appearing to be maximal when SRP concentrations are

around 10–50 nM [*Lomas et al.*, 2010; *Wurl et al.*, 2013; *Mahaffey et al.*, 2014]. Within the NASG, relative to the bulk community, *Trichodesmium* appears to be a better competitor for phosphomonoesters than for DIP [*Orchard et al.*, 2010].

Differences in mortality might also be expected to influence R^* (equations (1) and (2)). Thus, for example, any reduced grazing pressure on the colonial *Trichodesmium* relative to competing unicellular diazotrophs would have a tendency to lower both R^*_P and R^*_{Fe} for the former (equations (1) and (2)). Considering competition between *Trichodesmium* and unicellular diazotrophs from this perspective, it is thus interesting to speculate whether lowered mortality could contribute to *Trichodesmium* having a lower R^*_P and hence being the better competitor for P, while higher overall Fe requirements for *Trichodesmium* [*Berman-Frank et al.*, 2007] may be insufficient to offset any lowered mortality in the case of R^*_{Fe}, leaving unicellular diazotrophs as better competitors for Fe.

Potential differences in relative mortality rates, Fe requirements, P requirements, and P uptake mechanisms could hence all be argued to result in *Trichodesmium* being the best diazotrophic competitor for P (lowest R^*_P), while unicellular diazotrophs are better competitors for Fe (lower R^*_{Fe}). Dominance of *Trichodesmium* in the low P-high Fe regime of the NASG (Figure 9a) and non-*Trichodesmium* diazotrophs in the SASG would be consistent with such suggestions. Consistent with previous work [*Monteiro et al.*, 2010], modification of the simple numerical model to include two diazotrophs illustrates these arguments (Figure 10). Specifically, the simple model extension results in dominance of a putative *Trichodesmium*-type diazotroph along the R^*_P arm, with a putative non-*Trichodesmium* type along the R^*_{Fe} arm (Figure 10), when the former are assumed to be the better P competitor and poorer Fe competitor. In this regard the western SASG may be analogous to the Pacific Ocean, where P* values are elevated and DFe concentrations may be reduced [*Martino et al.*, 2014], creating an environment where unicellular diazotrophs are often able to outcompete *Trichodesmium* for the available Fe [*Monteiro et al.*, 2010].

More generally, both taxonomic and stoichiometric diversity within natural systems would in reality tend to result in multiple R^* values representing a diverse and complex diazotroph community [*Monteiro et al.*, 2010]. Moreover, away from the dominant large atmospheric sources of dust from North Africa [*Conway and John*, 2014], other Fe inputs including sedimentary [*Moore and Braucher*, 2008] and hydrothermal [*Saito et al.*, 2013] may need to be considered. For example, the argued depletion of P^* due to significant diazotrophy in the western South Atlantic gyre (Figures 4c and 4d) may result from a combination of Patagonian dust inputs or sedimentary inputs from the eastern South American shelf. However, the emergent qualitative relationships we highlight between limiting nutrients are generally expected to be robust to complexities including diversity of Fe source, diazotroph community, and stoichiometric variability [*Monteiro et al.*, 2010; *Ward et al.*, 2013].

3.4. Implications for Scales of N-P Coupling

In order to prevent large swings in oceanic productivity, feedback mechanisms are assumed to couple the N and P cycles over sufficiently large time and space scales [*Falkowski*, 1997; *Tyrrell*, 1999]. The scales over which this coupling operates are a crucial determinant of potential variability in the oceanic N inventory and are likely dictated by the significance of any environmental drivers of diazotrophy beyond the supply of excess P [*Codispoti*, 2007; *Deutsch et al.*, 2007; *Moore et al.*, 2009; *Weber and Deutsch*, 2014]. Our compiled observational data set indicating significant diazotrophy within both the NASG and SASG (Figures 2c, 3e, 4, 5a and 5b), alongside the presence of at least some areas of depleted P (~0 P*) in both gyres (Figures 2a, 4c, and 4k), is consistent with the dominance of regional scale coupling indicated by recent data constrained modeling [*Weber and Deutsch*, 2014]. However, observed relationships between DFe, DIP (alongside DOP and TDP), and patterns of diazotrophy also suggest significant local-regional scale controls on diazotrophy beyond excess P supply alone (Figure 9). Moreover, a degree of decoupling between local fixed N loss and N_2 fixation is apparent in the Atlantic, particularly in the NASG, where external inputs of P* appear to be required to sustain diazotrophy [*Moore et al.*, 2009; *Palter et al.*, 2010]. Although the estimated extent of decoupling in the Atlantic is minor in global terms, being $<$15% of the global fixed N budget [*Moore et al.*, 2009], the observed high rates of diazotrophy in the southern region of the NASG remain indicative of some degree of decoupling at local through to basin scales, as is likely necessary in order to prevent strong positive feedback on fixed N loss in oceanic oxygen minimum zones [*Canfield*, 2006; *Landolfi et al.*, 2013].

As suggested by a range of modeling studies [*Monteiro et al.*, 2011; *Dutkiewicz et al.*, 2012; *Ward et al.*, 2013; *Dutkiewicz et al.*, 2014], dual Fe-P control on diazotrophy [*Falkowski*, 1997; *Wu et al.*, 2000; *Moore et al.*, 2009; *Schlosser et al.*, 2014], as further supported by the current study (Figures 2 and 9), generates the potential for altered patterns of N_2 fixation under a range of global change scenarios. For example, within the regions of significant excess P* in the low Fe eastern SASG, altered patterns or even magnitudes of diazotrophy might be expected under altered Fe or macronutrient inputs [*Dutkiewicz et al.*, 2014]. Moreover, given the potential importance of southern sourced mode/intermediate waters for P* supply to the north [*Moore et al.*, 2009; *Palter et al.*, 2010; *Straub et al.*, 2013], any hypothetical alterations to diazotrophy in the SASG might be expected to result in opposite and potentially compensatory changes in N_2 fixation within the NASG. The potential for multiple environmental controls (e.g., P, Fe, temperature, and pCO_2) on diazotrophs, as indicated here (Figures 7 and 9) and further suggested by culture studies [*Breitbarth et al.*, 2007; *Hutchins et al.,* 2007, 2013; *Fu et al.*, 2014], thus requires that patterns of N_2 fixation and diazotroph biogeography, alongside the potential for these to change, be interpreted with an integrative understanding of both local and far field effects.

4. Conclusion

Here we present a comprehensive observation-based assessment describing the realized niche of diazotrophs in general and *Trichodesmium* in particular within the (sub)tropical Atlantic. We interpret the prevailing Fe and P biogeochemistry of the region in terms of the well-established resource ratio framework [*Dutkiewicz et al.*, 2012; *Ward et al.*, 2013]. In doing so, we present further evidence supporting distinct diazotrophic provinces [*Ward et al.*, 2013] along observed antithetical Fe and P gradients. Such gradients appear to manifest at basin scales between the eastern and western SASG and interbasin scales between the SASG and NASG. Highlighting a distinct lack of correlation between any one proposed environmental driving parameter (SST, pCO_2, DIP, or DFe) and diazotrophic activity and abundances, we emphasize how simple conceptual arguments and idealized numerical models assuming dual control by Fe and P supply are entirely consistent with available observations. In particular, we suggest that observed L-shaped relationships between DFe and DIP in the Atlantic are both a consequence of and diagnostic of diazotroph-Fe-P feedback. By implication, the lack of such a relationship, if sampled over a sufficient range of ratios for total Fe and P supply, would have provided evidence for the absence of nutrient control and hence presumably dominance of other drivers of diazotrophy and reciprocally a reduced influence of diazotrophy on observed Fe and P distributions. Hence, while SST and pCO_2 may have an observed physiological effect on diazotroph and specifically *Trichodesmium* growth rates [*Breitbarth et al.*, 2007; *Hutchins et al.,* 2007, 2013; *Fu et al.*, 2014], in the extant (sub)tropical Atlantic these effects are apparently overridden by nutrient (P and Fe) availability. These findings support the suggestion [*Dutkiewicz et al.*, 2014] that the resource ratio framework likely provides a strong basis for interpretation of past [*Straub et al.*, 2013] or predicted future changes [*Luo et al.*, 2013; *Dutkiewicz et al.*, 2014; *Weber and Deutsch*, 2014] in diazotrophy.

Acknowledgments

The data presented in this paper are available from either the British Oceanographic Data Centre (http://www.bodc.ac.uk/) or directly from J.T. Snow (j.snow@noc.soton.ac.uk). The work was supported by the UK Natural Environment Research Council through a grant to the University of Southampton (NE/G015732/1) and National Capability funding to the Plymouth Marine Laboratory and the National Oceanography Centre, Southampton. The study is a UK contribution to the international SOLAS, GEOTRACES, and IMBER projects. This is contribution number 260 of the AMT program. We would like to thank D. Baker, S. Reynolds, V. Kitidis, D. Honey, E. Tynan, S. Ussher, M. Patey, M. Rijenkenberg, S. Torres Valdes, U. Schuster, F. Malien, H. Luger, P. Fritsche, A. Kortzinger, P. Croot, C. Dumousseaud, and B. Ward for their contributions toward data collection and discussion and two anonymous referees for their comments.

References

Barcelos e Ramos, J., H. Biswas, K. G. Schulz, J. LaRoche, and U. Riebesell (2007), Effect of rising atmospheric carbon dioxide on the marine nitrogen fixer Trichodesmium, *Global Biogeochem. Cycles*, *21*, GB2028, doi:10.1029/2006GB002898.

Berman-Frank, I., P. Lundgren, Y. B. Chen, H. Küpper, Z. Kolber, B. Bergman, and P. Falkowski (2001), Segregation of nitrogen fixation and oxygenic photosynthesis in the marine cyanobacterium Trichodesmium, *Science*, *294*(5546), 1534–1537, doi:10.1126/science.1064082.

Berman-Frank, I., A. Quigg, Z. V. Finkel, A. J. Irwin, and L. Haramaty (2007), Nitrogen-fixation strategies and Fe requirements in cyanobacteria, *Limnol. Oceangr.*, *52*(5), 2260–2269, doi:10.4319/lo.2007.52.5.2260.

Böttjer, D., D. M. Karl, R. M. Letelier, D. A. Viviani, and M. J. Church (2014), Experimental assessment of diazotroph responses to elevated seawater pCO_2 in the North Pacific subtropical gyre, *Global Biogeochem. Cycles*, *28*, 601–616, doi:10.1002/2013GB004690.

Bowie, A. R., D. J. Whitworth, E. P. Achterberg, R. Mantoura, and P. J. Worsfold (2002), Biogeochemistry of Fe and other trace elements (Al, Co, Ni) in the upper Atlantic Ocean, *Deep Sea Res., Part I*, *49*(4), 605–636, doi:10.1016/s0967-0637(01)00061-9.

Boyd, P. W., K. A. Hunter, G. A. Jackson, E. Ibisanmi, E. Ibisanmi, S. G. Sander, and S. G. Sander (2010), Remineralization of upper ocean particles: Implications for iron biogeochemistry, *Limnol. Oceangr.*, *55*(3), 1271–1288, doi:10.4319/lo.2010.55.3.1271.

Breitbarth, E., A. Oschlies, and J. LaRoche (2007), Physiological constraints on the global distribution of Trichodesmium—Effect of temperature on diazotrophy, *Biogeosciences*, *4*(1), 53–61, doi:10.5194/bg-4-53-2007.

Brewer, P. G., and J. P. Riley (1965), The automatic determination of nitrate in seawater, *Deep Sea Res. Oceanogr. Abstr.*, *12*(6), 765–772, doi:10.1016/0011-7471(65)90797-7.

Broecker, W. S., and G. M. Henderson (1998), The sequence of events surrounding Termination II and their implications for the cause of glacial-interglacial CO_2 changes, *Paleoceanography*, *13*(4), 352–364, doi:10.1029/98PA00920.

Canfield, D. E. (2006), Models of oxic respiration, denitrification and sulfate reduction in zones of coastal upwelling, *Geochim. Cosmochim. Acta*, *70*(23), 5753–5765, doi:10.1016/j.gca.2006.07.023.

Capone, D. G., J. A. Burns, J. P. Montoya, A. Subramaniam, C. Mahaffey, T. Gunderson, A. F. Michaels, and E. J. Carpenter (2005), Nitrogen fixation by Trichodesmium spp.: An important source of new nitrogen to the tropical and subtropical North Atlantic Ocean, *Global Biogeochem. Cycles*, *19*, GB2024, doi:10.1029/2004GB002331.

Carpenter, E. J., A. Subramaniam, and D. G. Capone (2004), Biomass and primary productivity of the cyanobacterium Trichodesmium spp. in the tropical N Atlantic ocean, *Deep Sea Res., Part I*, *51*(2), 173–203, doi:10.1016/j.dsr.2003.10.006.

Carvalho, M., S. M. F. Gianesella, and F. M. P. Saldanha-Corrêa (2008), Trichodesmium erythraeum Bloom on the Continental Shelf off Santos, Southeast Brazil, *Braz. J. Oceanogr.*, *56*(4), 307–311, doi:10.1590/S1679-87592008000400006.

Codispoti, L. A. (2007), An oceanic fixed nitrogen sink exceeding 400 Tg N a^{-1} vs the concept of homeostasis in the fixed-nitrogen inventory, *Biogeosciences*, *4*(2), 233–253.

Conway, T. M., and S. G. John (2014), Quantification of dissolved iron sources to the North Atlantic Ocean, *Nature*, *511*(7508), 212–215, doi:10.1038/nature13482.

Croot, P. L., P. Streu, and A. R. Baker (2004), Short residence time for iron in surface seawater impacted by atmospheric dry deposition from Saharan dust events, *Geophys. Res. Lett.*, *31*, L23S08, doi:10.1029/2004GL020153.

Cullen, J. J. (1991), Hypotheses to explain high-nutrient conditions in the open sea, *Limnol. Oceangr.*, *36*(8), 1578–1599, doi:10.4319/lo.1991.36.8.1578.

Dabundo, R., M. F. Lehmann, L. Treibergs, C. R. Tobias, M. A. Altabet, P. H. Moisander, and J. Granger (2014), The contamination of commercial $^{15}N_2$ gas stocks with ^{15}N-labeled nitrate and ammonium and consequences for nitrogen fixation measurements, *PLoS One*, *9*(10), e110335, doi:10.1371/journal.pone.0110335.

Deutsch, C., J. L. Sarmiento, D. M. Sigman, N. Gruber, and J. P. Dunne (2007), Spatial coupling of nitrogen inputs and losses in the ocean, *Nature*, *445*(7124), 163–167, doi:10.1038/nature05392.

Dickson, A. G., C. L. Sabine, and J. R. Christian (2007), Guide to best practices for ocean CO_2 measurements, PICES Special Publisher.

Duce, R. A., et al. (2008), Impacts of atmospheric anthropogenic nitrogen on the open ocean, *Science*, *320*(5878), 893–897, doi:10.1126/science.1150369.

Dutkiewicz, S., M. J. Follows, and J. G. Bragg (2009), Modeling the coupling of ocean ecology and biogeochemistry, *Global Biogeochem. Cycles*, *23*, GB3017, doi:10.1029/2008GB003405.

Dutkiewicz, S., B. A. Ward, F. Monteiro, and M. J. Follows (2012), Interconnection of nitrogen fixers and iron in the Pacific Ocean: Theory and numerical simulations, *Global Biogeochem. Cycles*, *26*, GB1012, doi:10.1029/2011GB004039.

Dutkiewicz, S., B. A. Ward, J. R. Scott, and M. J. Follows (2014), Understanding predicted shifts in diazotroph biogeography using resource competition theory, *Biogeosciences*, *11*, 5445–5461, doi:10.5194/bg-11-5445-2014.

Dyhrman, S. T., P. D. Chappell, S. T. Haley, J. W. Moffett, E. D. Orchard, J. B. Waterbury, and E. A. Webb (2006), Phosphonate utilization by the globally important marine diazotroph Trichodesmium, *Nature*, *439*(7072), 68–71, doi:10.1038/nature04203.

Falkowski, P. G. (1997), Evolution of the nitrogen cycle and its influence on the biological sequestration of CO_2 in the ocean, *Nature*, *387*(6630), 272–275, doi:10.1038/387272a0.

Fernandez, A., B. Mouriño-Carballido, A. Bode, M. Varela, and E. Maranon (2010), Latitudinal distribution of *Trichodesmium* spp. and N_2 fixation in the Atlantic Ocean, *Biogeosciences*, *7*(10), 3167–3176, doi:10.5194/bg-7-3167-2010.

Foster, R. A., A. Subramaniam, C. Mahaffey, E. J. Carpenter, D. G. Capone, and J. P. Zehr (2007), Influence of the Amazon River plume on distributions of free-living and symbiotic cyanobacteria in the western tropical North Atlantic Ocean, *Limnol. Oceangr.*, *52*(2), 517–532, doi:10.4319/lo.2007.52.2.0517.

Fu, F. X., E. Yu, N. S. Garcia, J. Gale, Y. Luo, E. A. Webb, and D. A. Hutchins (2014), Differing responses of marine N_2 fixers to warming and consequences for future diazotroph community structure, *Aquat. Microb. Ecol.*, *72*(1), 33–46, doi:10.3354/ame01683.

Garcia, N. S., F. X. Fu, and D. A. Hutchins (2013), Colimitation of the unicellular photosynthetic diazotroph Crocosphaera watsonii by phosphorus, light, and carbon dioxide, *Limnol. Oceanogr.*, *58*(4), 1501–1512.

Garcia, N. S., F. Fu, P. N. Sedwick, and D. A. Hutchins (2015), Iron deficiency increases growth and nitrogen-fixation rates of phosphorus-deficient marine cyanobacteria, *ISME J.*, *9*(1), 238–245, doi:10.1038/ismej.2014.104.

Goebel, N. L., K. A. Turk, K. M. Achilles, R. Paerl, I. Hewson, A. E. Morrison, J. P. Montoya, C. A. Edwards, and J. P. Zehr (2010), Abundance and distribution of major groups of diazotrophic cyanobacteria and their potential contribution to N_2 fixation in the tropical Atlantic Ocean, *Environ. Microbiol.*, *12*(12), 3272–3289, doi:10.1111/j.1462-2920.2010.02303.x.

Gradoville, M. R., A. E. White, D. Böttjer, and M. J. Church (2014), Diversity trumps acidification: Lack of evidence for carbon dioxide enhancement of Trichodesmium community nitrogen or carbon fixation at Station ALOHA, *Limnol. Oceanogr.*, *59*(3), 645–659.

Grasshoff, K., K. Kremling, and M. Ehrhardt (1976), *Methods of Seawater Analysis*, John Wiley.

Graziano, L. M., R. J. Geider, W. Li, and M. Olaizola (1996), Nitrogen limitation of North Atlantic phytoplankton: Analysis of physiological condition in nutrient enrichment experiments, *Aquat. Microb. Ecol.*, *11*(1), 53–64, doi:10.3354/ame011053.

Großkopf, T., W. Mohr, T. Baustian, H. Schunck, D. Gill, M. M. M. Kuypers, G. Lavik, R. A. Schmitz, D. W. R. Wallace, and J. LaRoche (2012), Doubling of marine dinitrogen-fixation rates based on direct measurements, *Nature*, *488*(7411), 361–364, doi:10.1038/nature11338.

Gruber, N. (2008), *The Marine Nitrogen Cycle*, Elsevier.

Hardman-Mountford, N. J., et al. (2008), An operational monitoring system to provide indicators of CO_2-related variables in the ocean, *ICES J. Mar. Sci.*, *65*(8), 1498–1503, doi:10.1093/icesjms/fsn110.

Huertas, I. E., M. Rouco, V. López-Rodas, and E. Costas (2011), Warming will affect phytoplankton differently: Evidence through a mechanistic approach, *Proc. Biol. Sci.*, *278*(1724), 3534–3543, doi:10.1098/rspb.2011.0160.

Hutchins, D. A., F. X. Fu, Y. Zhang, M. E. Warner, Y. Feng, K. Portune, P. W. Bernhardt, and M. R. Mulholland (2007), CO_2 control of Trichodesmium N_2 fixation, photosynthesis, growth rates, and elemental ratios: Implications for past, present, and future ocean biogeochemistry, *Limnol. Oceangr.*, *52*(4), 1293–1304, doi:10.4319/lo.2007.52.4.1293.

Hutchins, D. A., F.-X. Fu, E. A. Webb, N. Walworth, and A. Tagliabue (2013), Taxon-specific response of marine nitrogen fixers to elevated carbon dioxide concentrations, *Nat. Geosci.*, *6*(9), 790–795, doi:10.1038/ngeo1858.

Jickells, T. (2006), The role of air-sea exchange in the marine nitrogen cycle, *Biogeosciences*, *3*(3), 271–280, doi:10.5194/bg-3-271-2006.

Jickells, T. D., et al. (2005), Global iron connections between desert dust, ocean biogeochemistry, and climate, *Science*, *308*(5718), 67–71, doi:10.1126/science.1105959.

Kitidis, V., et al. (2012), Seasonal dynamics of the carbonate system in the Western English Channel, *Cont. Shelf Res.*, *42*, 30–40, doi:10.1016/j.csr.2012.04.012.

Klunder, M. B., P. Laan, R. Middag, H. J. W. De Baar, and J. C. van Ooijen (2011), Dissolved iron in the Southern Ocean (Atlantic sector), *Deep Sea Res. Part II: Top. Stud. Oceanogr.*, *58*(25–26), 2678–2694, doi:10.1016/j.dsr2.2010.10.042.

Körtzinger, A. (1999), *Determination of Carbon Dioxide Partial Pressure (p(CO_2))*, Wiley-VCH Verlag GmbH, Weinheim, Germany.
Kranz, S. A., D. Sültemeyer, K.-U. Richter, and B. Rost (2009), Carbon acquisition by Trichodesmium: The effect of pCO_2 and diurnal changes, *Limnol. Oceangr.*, *54*(2), 548–559, doi:10.4319/lo.2009.54.2.0548.
Kranz, S. A., D. Wolf-Gladrow, G. Nehrke, G. Langer, and B. Rost (2010), Calcium carbonate precipitation induced by the growth of the marine cyanobacteria Trichodesmium, *Limnol. Oceangr.*, *55*(6), 2563–2569, doi:10.4319/lo.2010.55.6.2563.
Landolfi, A., H. Dietze, W. Koeve, and A. Oschlies (2013), Overlooked runaway feedback in the marine nitrogen cycle: The vicious cycle, *Biogeosciences*, *10*(3), 1351–1363, doi:10.5194/bg-10-1351-2013.
LaRoche, J., and E. Breitbarth (2005), Importance of the diazotrophs as a source of new nitrogen in the ocean, *J. Sea Res.*, *53*(1–2), 67–91, doi:10.1016/j.seares.2004.05.005.
Lomas, M. W., A. L. Burke, D. A. Lomas, D. W. Bell, C. Shen, S. T. Dyhrman, and J. W. Ammerman (2010), Sargasso Sea phosphorus biogeochemistry: An important role for dissolved organic phosphorus (DOP), *Biogeosciences*, *7*(2), 695–710, doi:10.5194/bg-7-695-2010.
Luo, Y. W., et al. (2012), Database of diazotrophs in global ocean: Abundance, biomass and nitrogen fixation rates, *Earth Syst. Sci. Data*, *4*(1), 47–73, doi:10.5194/essd-4-47-2012.
Luo, Y. W., I. D. Lima, D. M. Karl, and S. C. Doney (2013), Data-based assessment of environmental controls on global marine nitrogen fixation, *Biogeosci. Discuss.*, *10*(4), 7367–7412, doi:10.5194/bgd-10-7367-2013.
Mahaffey, C., A. F. Michaels, and D. G. Capone (2005), The conundrum of marine N_2 fixation, *Am. J. Sci.*, *305*(6–8), 546–595, doi:10.2475/ajs.305.6-8.546.
Mahaffey, C., S. Reynolds, C. E. Davis, and M. C. Lohan (2014), Alkaline phosphatase activity in the subtropical ocean: Insights from nutrient, dust and trace metal addition experiments, *Front. Mar. Sci.*, *1*, doi:10.3389/fmars.2014.00073.
Mahowald, N. M., A. R. Baker, G. Bergametti, N. Brooks, R. A. Duce, T. D. Jickells, N. Kubilay, J. M. Prospero, and I. Tegen (2005), Atmospheric global dust cycle and iron inputs to the ocean, *Global Biogeochem. Cycles*, *19*, GB4025, doi:10.1029/2004GB002402.
Martino, M., D. Hamilton, A. R. Baker, T. D. Jickells, T. Bromley, Y. Nojiri, B. Quack, and P. W. Boyd (2014), Western Pacific atmospheric nutrient deposition fluxes, their impact on surface ocean productivity, *Global Biogeochem. Cycles*, *28*, 712–728, doi:10.1002/2013GB004794.
Mather, R. L., S. E. Reynolds, G. A. Wolff, S. Torres-Valdes, E. M. S. Woodward, A. Landolfi, X. Pan, R. Sanders, and E. P. Achterberg (2008), Phosphorus cycling in the North and South Atlantic Ocean subtropical gyres, *Nat. Geosci.*, *1*(7), 439–443, doi:10.1038/ngeo232.
McLaughlin, K., J. A. Sohm, G. A. Cutter, M. W. Lomas, and A. Paytan (2013), Phosphorus cycling in the Sargasso Sea: Investigation using the oxygen isotopic composition of phosphate, enzyme-labeled fluorescence, and turnover times, *Global Biogeochem. Cycles*, *27*, 375–387, doi:10.1002/gbc.20037.
Mills, M. M., C. Ridame, M. Davey, J. La Roche, and R. J. Geider (2004), Iron and phosphorus co-limit nitrogen fixation in the eastern tropical North Atlantic, *Nature*, *429*(6989), 292–294, doi:10.1038/nature02550.
Milne, A., W. Landing, M. Bizimis, and P. Morton (2010), Determination of Mn, Fe, Co, Ni, Cu, Zn, Cd and Pb in seawater using high resolution magnetic sector inductively coupled mass spectrometry (HR-ICP-MS), *Anal. Chim. Acta*, *665*(2), 200–207, doi:10.1016/j.aca.2010.03.027.
Mitchell, T. P., and J. M. Wallace (1992), The annual cycle in equatorial convection and sea surface temperature, *J. Clim.*, *5*(10), 1140–1156, doi:10.1175/1520-0442(1992)005<1140:taciec>2.0.co;2.
Mohr, W., T. Großkopf, D. W. R. Wallace, and J. LaRoche (2010), Methodological underestimation of oceanic nitrogen fixation rates, *PLoS One*, *5*(9), doi:10.1371/journal.pone.0012583.
Moisander, P. H., R. A. Beinart, I. Hewson, A. E. White, K. S. Johnson, C. A. Carlson, J. P. Montoya, and J. P. Zehr (2010), Unicellular cyanobacterial distributions broaden the oceanic N_2 fixation domain, *Science*, *327*(5972), 1512–1514, doi:10.1126/science.1185468.
Monteiro, F. M., M. J. Follows, and S. Dutkiewicz (2010), Distribution of diverse nitrogen fixers in the global ocean, *Global Biogeochem. Cycles*, *24*, GB3017, doi:10.1029/2009GB003731.
Monteiro, F. M., S. Dutkiewicz, and M. J. Follows (2011), Biogeographical controls on the marine nitrogen fixers, *Global Biogeochem. Cycles*, *25*, GB2003, doi:10.1029/2010GB003902.
Montoya, J. P., M. Voss, P. Kahler, and D. G. Capone (1996), A simple, high-precision, high-sensitivity tracer assay for N_2 fixation, *Appl. Environ. Microbiol.*, *62*(3), 986–993.
Montoya, J. P., C. M. Holl, J. P. Zehr, A. Hansen, T. A. Villareal, and D. G. Capone (2004), High rates of N_2 fixation by unicellular diazotrophs in the oligotrophic Pacific Ocean, *Nature*, *430*(7003), 1027–1032, doi:10.1038/nature02824.
Moore, C. M., M. M. Mills, A. Milne, R. Langlois, E. P. Achterberg, K. Lochte, R. J. Geider, and J. La Roche (2006), Iron limits primary productivity during spring bloom development in the central North Atlantic, *Global Change Biol.*, *12*(4), 626–634, doi:10.1111/j.1365-2486.2006.01122.x.
Moore, C. M., M. M. Mills, R. Langlois, A. Milne, E. P. Achterberg, J. La Roche, and R. J. Geider (2008), Relative influence of nitrogen and phosphorous availability on phytoplankton physiology and productivity in the oligotrophic subtropical North Atlantic Ocean, *Limnol. Oceangr.*, *53*(1), 291–305, doi:10.4319/lo.2008.53.1.0291.
Moore, C. M., et al. (2009), Large-scale distribution of Atlantic nitrogen fixation controlled by iron availability, *Nat. Geosci.*, *2*(12), 867–871, doi:10.1038/ngeo667.
Moore, C. M., et al. (2013), Processes and patterns of oceanic nutrient limitation, *Nat. Geosci.*, *6*, 701–710.
Moore, J. K., and O. Braucher (2008), Sedimentary and mineral dust sources of dissolved iron to the world ocean, *Biogeosciences*, *5*(3), 631–656.
Moore, R. M., M. Kienast, M. Fraser, J. J. Cullen, C. Deutsch, S. Dutkiewicz, M. J. Follows, and C. J. Somes (2014), Extensive hydrogen supersaturations in the western South Atlantic Ocean suggest substantial underestimation of nitrogen fixation, *J. Geophys. Res. Oceans*, *119*, 4340–4350, doi:10.1002/2014JC010017.
Orchard, E. D., E. A. Webb, and S. T. Dyhrman (2009), Molecular analysis of the phosphorus starvation response in Trichodesmium spp., *Environ. Microbiol.*, *11*(9), 2400–2411, doi:10.1111/j.1462-2920.2009.01968.x.
Orchard, E. D., C. R. Benitez-Nelson, P. J. Pellechia, M. W. Lomas, and S. T. Dyhrman (2010), Polyphosphate in Trichodesmium from the low-phosphorus Sargasso Sea, *Limnol. Oceangr.*, *55*(5), 2161–2169, doi:10.4319/lo.2010.55.5.2161.
Palter, J. B., J. L. Sarmiento, and A. Gnanadesikan (2010), Fueling export production: Nutrient return pathways from the deep ocean and their dependence on the meridional overturning circulation, *Biogeosciences*, *7*(11), 3549–3568, doi:10.5194/bg-7-3549-2010.
Pandey, K. D., S. P. Shukla, P. N. Shukla, D. D. Giri, J. S. Singh, P. Singh, and A. K. Kashyap (2004), Cyanobacteria in Antarctica: Ecology, physiology and cold adaptation, *Cell. Mol. Biol. (Noisy-le-grand)*, *50*(5), 575–584.
Patey, M. D., M. J. A. Rijkenberg, P. J. Statham, M. C. Stinchcombe, E. P. Achterberg, and M. Mowlem (2008), Determination of nitrate and phosphate in seawater at nanomolar concentrations, *TrAC, Trends Anal. Chem.*, *27*(2), 169–182, doi:10.1016/j.trac.2007.12.006.
Philander, S. G. H., D. Gu, G. Lambert, T. Li, D. Halpern, N.-C. Lau, and R. C. Pacanowski (1996), Why the ITCZ is mostly north of the equator, *J. Clim.*, *9*(12), 2958–2972, doi:10.1175/1520-0442(1996)009<2958:wtiimn>2.0.co;2.
Raven, J. A. (1988), The iron and molybdenum use efficiencies of plant growth with different energy, carbon and nitrogen sources, *New Phytol.*, *109*(3), 279–287, doi:10.1111/j.1469-8137.1988.tb04196.x.

Reynolds, S., C. Mahaffey, V. Roussenov, and R. G. Williams (2014), Evidence for production and lateral transport of dissolved organic phosphorus in the eastern subtropical North Atlantic, *Global Biogeochem. Cycles*, *28*, 805–824, doi:10.1002/2013GB004801.

Richier, S., A. I. Macey, N. J. Pratt, D. J. Honey, C. M. Moore, and T. S. Bibby (2012), Abundances of iron-binding photosynthetic and nitrogen-fixing proteins of Trichodesmium both in culture and in situ from the North Atlantic., edited by L. J. Stal, *PLoS One*, *7*(5), e35571, doi:10.1371/journal.pone.0035571.

Rijkenberg, M. J. A., S. Steigenberger, C. F. Powell, H. van Haren, M. D. Patey, A. R. Baker, and E. P. Achterberg (2012), Fluxes and distribution of dissolved iron in the eastern (sub-) tropical North Atlantic Ocean, *Global Biogeochem. Cycles*, *26*, GB3004, doi:10.1029/2011GB004264.

Rödenbeck, C., R. F. Keeling, D. C. E. Bakker, N. Metzl, C. Sabine, and M. Heimann (2013), Global surface-ocean pCO_2 and sea–air CO_2 flux variability from an observation-driven ocean mixed-layer scheme, *Ocean Sci.*, *9*(2), 193–216, doi:10.5194/os-9-193-2013.

Roy, N. K., R. K. Ghosh, and J. Das (1982), Monomeric alkaline phosphatase of Vibrio cholerae, *J. Bacteriol.*, *150*(3), 1033–1039.

Ryther, J. H., and W. M. Dunstan (1971), Nitrogen, phosphorus, and eutrophication in the coastal marine environment, *Science*, *171*(3975), 1008–1013, doi:10.1126/science.171.3975.1008.

Saito, M. A., S. Dutkiewicz, V. V. Bulygin, D. M. Moran, M. J. Follows, and J. B. Waterbury (2011), Iron conservation by reduction of metalloenzyme inventories in the marine diazotroph Crocosphaera watsonii, *Proc. Natl. Acad. Sci. U.S.A.*, *108*(6), 2184–2189, doi:10.1073/pnas.1006943108.

Saito, M. A., A. E. Noble, A. Tagliabue, T. J. Goepfert, C. H. Lamborg, and W. J. Jenkins (2013), Slow-spreading submarine ridges in the South Atlantic as a significant oceanic iron source, *Nat. Geosci.*, *6*(9), 775–779, doi:10.1038/ngeo1893.

Sandh, G., R. El-Shehawy, B. Díez, and B. Bergman (2009), Temporal separation of cell division and diazotrophy in the marine diazotrophic cyanobacterium Trichodesmium erythraeum IMS101, *FEMS Microbiol. Lett.*, *295*(2), 281–288, doi:10.1111/j.1574-6968.2009.01608.x.

Sañudo-Wilhelmy, S. A., A. B. Kustka, C. J. Gobler, D. A. Hutchins, M. Yang, K. Lwiza, J. Burns, D. G. Capone, J. A. Raven, and E. J. Carpenter (2001), Phosphorus limitation of nitrogen fixation by Trichodesmium in the central Atlantic Ocean, *Nature*, *411*(6833), 66–69, doi:10.1038/35075041.

Schlosser, C., J. K. Klar, B. D. Wake, J. T. Snow, D. J. Honey, E. M. S. Woodward, M. C. Lohan, E. P. Achterberg, and C. M. Moore (2014), Seasonal ITCZ migration dynamically controls the location of the (sub)tropical Atlantic biogeochemical divide, *Proc. Natl. Acad. Sci. U.S.A.*, *111*(4), 1438–1442, doi:10.1073/pnas.1318670111.

Shi, T., Y. Sun, and P. G. Falkowski (2007), Effects of iron limitation on the expression of metabolic genes in the marine cyanobacterium *Trichodesmium erythraeum* IMS101, *Environ Microbiol.*, *9*(12), 2945–2956, doi:10.1111/j.1462-2920.2007.01406.x.

Sohm, J. A., C. Mahaffey, and D. G. Capone (2008), Assessment of relative phosphorus limitation of Trichodesmium spp. in the North Pacific, North Atlantic, and the north coast of Australia, *Limnol. Oceangr.*, *53*(6), 2495–2502, doi:10.4319/lo.2008.53.6.2495.

Sohm, J. A., A. Subramaniam, T. E. Gunderson, E. J. Carpenter, and D. G. Capone (2011a), Nitrogen fixation by Trichodesmium spp. and unicellular diazotrophs in the North Pacific Subtropical Gyre, *J. Geophys. Res.*, *116*, G03002, doi:10.1029/2010JG001513.

Sohm, J. A., E. A. Webb, and D. G. Capone (2011b), Emerging patterns of marine nitrogen fixation, *Nat. Rev. Microbiol.*, *9*(7), 499–508, doi:10.1038/nrmicro2594.

Sohm, J. A., J. A. Hilton, A. E. Noble, J. P. Zehr, M. A. Saito, and E. A. Webb (2011c), Nitrogen fixation in the South Atlantic Gyre and the Benguela Upwelling System, *Geophys. Res. Lett.*, *38*, L16608, doi:10.1029/2011GL048315.

Staal, M., F. J. R. Meysman, and L. J. Stal (2003), Temperature excludes N_2-fixing heterocystous cyanobacteria in the tropical oceans, *Nature*, *425*(6957), 504–507, doi:10.1038/nature01999.

Stal, L. J. (2009), Is the distribution of nitrogen-fixing cyanobacteria in the oceans related to temperature?, *Environ. Microbiol.*, *11*(7), 1632–1645, doi:10.1111/j.1758-2229.2009.00016.x.

Straub, M., D. M. Sigman, H. Ren, A. Martínez-García, A. N. Meckler, M. P. Hain, and G. H. Haug (2013), Changes in North Atlantic nitrogen fixation controlled by ocean circulation, *Nature*, *501*(7466), 200–203, doi:10.1038/nature12397.

Subramaniam, A., et al. (2008), Amazon River enhances diazotrophy and carbon sequestration in the tropical North Atlantic Ocean, *Proc. Natl. Acad. Sci. U.S.A.*, *105*(30), 10,460–10,465, doi:10.1073/pnas.0710279105.

Thomas, M. K., C. T. Kremer, C. A. Klausmeier, and E. Litchman (2012), A global pattern of thermal adaptation in marine phytoplankton, *Science*, *338*(6110), 1085–1088, doi:10.1126/science.1224836.

Tilman, D. (1980), Resources: A graphical-mechanistic approach to competition and predation, *Am. Nat.*, *116*(3), 362, doi:10.1086/283633.

Tilman, D., S. S. Kilham, and P. Kilham (1982), Phytoplankton community ecology: The role of limiting nutrients, *Annu. Rev. Ecol. Syst.*, *13*(1), 349–372, doi:10.1146/annurev.es.13.110182.002025.

Tyrrell, T. (1999), The relative influences of nitrogen and phosphorus on oceanic primary production, *Nature*, *400*(6744), 525–531, doi:10.1038/22941.

Tyrrell, T., E. Marañón, A. J. Poulton, D. S. Harbour, and E. M. S. Woodward (2003), Large-scale latitudinal distribution of Trichodesmium spp. in the Atlantic Ocean, *J. Plankton Res.*, *25*(4), 405–416, doi:10.1093/plankt/25.4.405.

Van Mooy, B. A. S., et al. (2009), Phytoplankton in the ocean use non-phosphorus lipids in response to phosphorus scarcity, *Nature*, *458*(7234), 69–72, doi:10.1038/nature07659.

Ward, B. A., S. Dutkiewicz, C. M. Moore, and M. J. Follows (2013), Iron, phosphorus, and nitrogen supply ratios define the biogeography of nitrogen fixation, *Limnol. Oceangr.*, *58*(6), 2059–2075, doi:10.4319/lo.2013.58.6.2059.

Weber, T., and C. Deutsch (2014), Local versus basin-scale limitation of marine nitrogen fixation, *Proc. Natl. Acad. Sci. U.S.A.*, *111*(24), 8741–8746, doi:10.1073/pnas.1317193111.

Wilson, S. T., Z. S. Kolber, S. Tozzi, J. P. Zehr, and D. M. Karl (2012), Nitrogen fixation, hydrogen cycling, and electron transport kinetics in trichodesmium erythraeum (Cyanobacteria) strain IMS1011, *J. Phycol.*, *48*(3), 595–606, doi:10.1111/j.1529-8817.2012.01166.x.

Wu, J., W. Sunda, E. A. Boyle, and D. M. Karl (2000), Phosphate depletion in the Western North Atlantic Ocean, *Science*, *289*(5480), 759–762, doi:10.1126/science.289.5480.759.

Wurl, O., L. Zimmer, and G. A. Cutter (2013), Arsenic and phosphorus biogeochemistry in the ocean: Arsenic species as proxies for P-limitation, *Limnol. Oceanogr.*, doi:10.4319/lo.2013.58.2.0729.

Xie, S.-P., and K. Saito (2001), Formation and variability of a northerly ITCZ in a hybrid coupled AGCM: Continental forcing and oceanic–atmospheric feedback*, *J. Clim.*, *14*(6), 1262–1276, doi:10.1175/1520-0442(2001)014<1262:favoan>2.0.co;2.

Zehr, J. P. (2011), Nitrogen fixation by marine cyanobacteria, *Trends Microbiol.*, *19*(4), 162–173, doi:10.1016/j.tim.2010.12.004.